Low Complexity Rotation Algorithm for Reducing PAPR in Partial Transmits Sequence

Thamer Alameri (alamery.thamer@gmail.com)
Iraqi Police College https://orcid.org/0000-0001-8521-9711
Nabeel ali
University of Kufa
Mothana Attiah
Middle Technical University
Mohammed Saad Talib
University of Babylon
Jawad Mezaal
University of Baghdad

Research Article

Keywords: PAPR, PTS, IL-PT, Ad-PTS, PR-PTS

Posted Date: March 16th, 2021

DOI: https://doi.org/10.21203/rs.3.rs-264221/v1

Low Complexity Rotation Algorithm for Reducing PAPR in Partial Transmits Sequence

Thamer Alameri[1,2], Nabeel Salih Ali[3], Mothana L. Attiah[2,4], Mohammed Saad Talib[5], Jawad Kadhim Mezaal[6]
[1]Department of Computer Engineering, University of Technology, Baghdad, Iraq.
[2]Police College of Iraq, Baghdad, Iraq.
[3]Information Technology Research and Development Centre, University of Kufa, Iraq.
[4]Department of Computer Engineering, Electrical Engineering Technical College, Middle Technical University, Baghdad, Iraq
[5]College of Administration and Economics, University of Babylon – Iraq
[6]State Company for Oil Projects (SCOP), Baghdad, Iraq

Corresponding Author: Thamer Alameri **Email:** Alamery.thamer@gmail.com

Abstract: High peak to average power ratio (PAPR) is considered as a prime challenge in orthogonal frequency division multiplexing. The partial transmits sequence (PTS) technique is one of the most effective methods for restraining the PAPR pattern. This study proposes a novel approach for enhancing PAPR reduction performance in a PTS by partitioning each subblock into two parts then exchanging the first sample with the last selection in each part of the subblock to generate a new partitioning scheme. The proposed algorithm is analysed and applied to typical traditional segmentation schemes, namely, the adjacent, interleaving and pseudo-random schemes. Moreover, simulation is conducted with two scenarios in which the number of subcarriers is set to 128 and 256. In both systems, the improved segmentation schemes demonstrate PAPR reduction performance that is superior to that of the traditional strategies. Furthermore, the computational complexity level of the enhanced adjusted PTS scheme is low compared with that of the conventional schemes.

Keywords: PAPR. PTS. IL-PT. Ad-PTS. PR-PTS.

1. Introduction

Recently, 5th generation (5G) networks have drawn increasing attention from industrial and academic researchers owing to the rapid growth of communication markets [1]. Several applications have been introduced in 5G networks to meet the new requirements, such as machine-to-machine, Internet of things and vehicle-to-vehicle communications [2]. Partial Transmit Sequence (PTS) is one of the promising methods to mitigate PAPR [3]. One of the most significant discussions on the partial transmit sequence (PTS) approach is that input data are segmented into several subblocks. A set of phase coefficients rotates the subblock samples before combining them once again to produce a group of picked signals. Lastly, the signal with a minimum peak to average power ratio (PAPR) level is selected for transmission [4]. Recently, researchers have examined the effects of subblock segmentation schemes on PAPR reduction levels. Specifically, Ibraheem et al. discussed the influence of varying

subblock lengths on the adjacent (Ad) partitioning scheme and found that fixed subblock lengths can realise PAPR reduction performance better than varying subblock lengths [5]. Vidya presented traditional partitioning schemes and compared their influence on PAPR reduction performance [6].

Moreover, the authors concluded that the pseudo-random (PR) method is the ideal scheme among the partitioning methods. Researchers have developed new segmentation schemes. For example, Xiao suggested a novel technique for enhancing PAPR reduction performance by copying PR subblocks in the time domain (TD) to increase candidate signals [7]. Hong presented a hybrid scheme for minimising high PAPR patterns by merging the PR-PTS and interleaving PTS (IL-PTS) scheme [8]. Meanwhile, Miao proposed a novel approach by combining the IL and PR schemes with the Hadamard matrix [9]. Moreover, Ibraheem introduced a new algorithm by combining the Ad-PTS and IL-PTS scheme to minimise PAPR values [5]. Jawhar attempted to acquaint new partitioning algorithms to improve PAPR reduction capacity compared with conventional methods [4]. However, a significant problem with the application of high PAPRs in OFDM systems involves incremental PAPR levels, which make the system works in a nonlinear region of the power amplifier (PA), thereby, deteriorating the bit error rate (BER) and signal spectrum effectiveness [10]. Nevertheless, most previous research avoids the PAPR challenge. Several algorithms have been suggested as practical solutions rather than large dynamic-range PAs, such as tone reservation, nonlinear companding transform [11], clipping and filtering [12], PTS [4], selective level mapping [13], and active constellation extension [14]. Among the PAPR reduction techniques, the PTS, which was suggested by Muller in 1997, is the most efficient reduction method [15]. The PTS algorithm can lessen PAPR values effectively by increasing the computational complexity (CC) of a system. However, discussions on the impact of segmentation schemes on PAPR are limited. The current study proposes three traditional segmentation schemes that are enhanced through the application of a new algorithm, namely, the rotation algorithm. The PAPR reduction capacity of the enhanced schemes is better than that of the conventional techniques. However, the CC of the enhanced strategies records different levels compared with that of the traditional schemes.

The rest of this paper is structured as follows: The PTS technique is explained in Section 2, and Section 3 analyses the PTS segmentation method. Section 4 introduces the proposed algorithm, and Section 5 discusses the results. Finally, Section 6 presents the conclusion of the study.

2. Partial Transmit Sequence (PTS) Technique

2.1 Peak to Average Power Ratio (PAPR) and PTS

In an OFDM system, baseband subcarriers are often modulated using an Inverse Fast Fourier transform (IFFT) algorithm. Hence, the OFDM signal is expressed as (Kim, 2016) in **Eq. 1** [16].

$$y(n) = \frac{1}{\sqrt{N}} \sum_{k=0}^{N-1} Y_k e^{j2\pi kn/N} \quad , 0 \leq n \leq N-1 \tag{1}$$

Where N. represents, and the number of subcarriers Also, $\{Y_k, k = [0, 1, \ldots, N-1]\}$ is a baseband signal in a complex representation after mapping by one of the modulation methods, such as quadrature amplitude modulation (QAM). The OFDM signal in the TD is produced by superpositioning multiple sinusoidal functions. Thus, the instantaneous power of individual samples may be increased several times more than the mean intensity of the signal [17]. Therefore, the envelope fluctuation of the OFDM signal drives the high PA to operate outside the linear region, thereby deteriorating the signal spectrum and BER performance of the system [18]. Therefore, PAPR is adopted to compute the fluctuation of the OFDM signal in the TD. Thus, PAPR is defined as the highest instant signal power divided by the average power and expressed in decibel (dB) as in **Eq. 2**.

$$PAPR = 10log_{10} \frac{max|y(n)|^2}{E\{|y(n)|^2\}} \tag{2}$$

Where the E{.} represents the expected value. The complementary cumulative distribution function (CCDF) is contributed to calculate the PAPR probability that exceeds a threshold value as in **Eq. (3)** [19]**.**

$$P_r[PAPR(y(n) \geq PAPR_0] = 1 - (1 - e^{-PAPR_0})^N \tag{3}$$

Where P_r represents the probability function, and $PAPR_0$ symbolises the threshold value. Besides, to increase the prissily of the PAPR computations, the oversampling factor (L) is generally used by setting (L-1) N zeros among the samples. Thus, the CCDF can be expressed as in **Eq. 4** [19].

$$P_r[PAPR(y(n) \geq PAPR_0] = 1 - (1 - e^{-PAPR_0})^{NL} \tag{4}$$

The PAPR problem should be resolved before the OFDM signal is transmitted. The PTS technique is among the methods that can diminish high PAPRs effectively. The mechanism of the PTS technique involves the partitioning of the input data symbol into V subblocks. Next, the N-IFFT block is utilised to modulate the N-subcarriers with the input data symbols. Subsequently, a group of phase coefficient vectors rotates the subcarriers

of each subblock to produce a set of candidate signals. Given the influence of the phase coefficients, the candidate signals will exhibit different PAPR value levels. Accordingly, the candidate signal that achieves a low PAPR is sent to the receiver side [20] as shown in **Figure 1**.

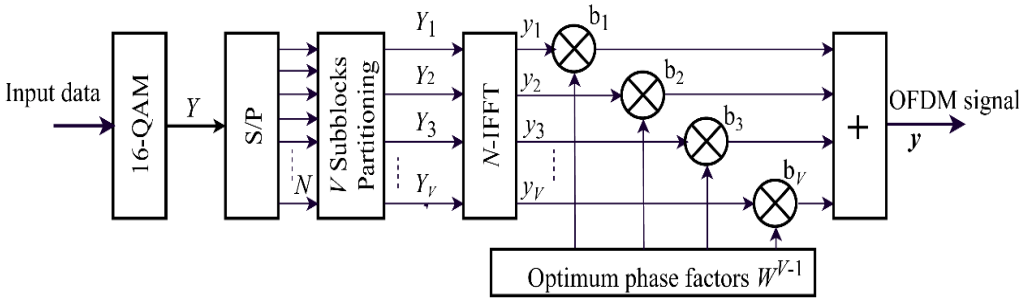

Figure. 1 C-PTS block diagram [21]

Figure 1 presents the simple scheme of the PTS approach, where 16-QAM maps the data symbol $Y_k = [Y_0, Y_1, \ldots, Y_{N-1}]$, and the complex data symbol is divided into V subsets $\{Y_V, v= 1, 2, \ldots, V\}$, as shown in **Eq. (5).**

$$Y_k = \sum_{v=1}^{V} Y_v \tag{5}$$

Next, the partitioned subblocks of the OFDM signal are multiplied by the phase rotation coefficients according to **Eq. (6)** as follows:

$$Y_k = \sum_{v=1}^{V} b_v Y_v \tag{6}$$

Where $\{b_v , v = 1, 2, \ldots, V\}$ is the phase coefficients. Afterwards, the IFFT operation is utilised to produce the OFDM signal, consequently; **Eq.7** expresses the output OFDM signal as:

$$y = \text{IFFT}\left\{\sum_{v=1}^{V} b_v Y_v\right\} \tag{7}$$

Equation (8) depicts the OFDM output signal due to linear characteristic of the IFFT function as follows:

$$y = \sum_{v=1}^{V} b_v \, \mathrm{IFFT}(Y_v) \tag{8}$$

In which,

$$y = \sum_{v=1}^{V} b_v \, y_v) \tag{9}$$

The optimum phase coefficient that drives the OFDM signal to attain the minimum PAPR value can be obtained by the following expression in **Eq. (10)** [22].

$$\{b_1, b_2, \ldots, b_V\} = \arg_{\{b_1, b_2, \ldots, b_V\}} \left(\min \left(max_{1 \le n \le N} \left\{ \left| \sum_{v=1}^{V} b_v \, Y_v \right| \right\} \right) \right) \tag{10}$$

Where arg(.) is the term that achieves the minimum PAPR value by setting the phase coefficient factors, furthermore, the optimum phase coefficient is obtained after (WV-1) attempts are performed, where W denotes the number of different phase coefficients, which is often limited to or for reducing the multiplication operations. Consequently, the PTS technique suffers from high computational complexity when determining the proper phase rotation coefficient. Furthermore, the receiver should recognise the index of the appropriate phase coefficient to recover the transmitted signal correctly. Hence, (log2WV-1) bits should be sent to the receiver by the transmitter as side information, which requires a portion of the bandwidth and can lead to the reduction of system capacity [23].

3. Segmentation Schemes

In the PTS technique, several subblocks are extracted by dividing the input data to reduce the high correlation level among the samples [24]. The partitioning input data sequence is the central part of the PTS technique; thus, the selection of a suitable partitioning scheme plays an essential role in mitigating the PAPR value. Three typical partitioning schemes are IL partitioning (IL-PTS), Ad partitioning (Ad-PTS) and PR partitioning (PR-PTS). The PAPR reduction gain of conventional schemes differs from one scheme to another. Furthermore, the partitioning operation must satisfy different conditions, such as subblocks must be equal in length, whereas the second concerning active subcarriers must not overlap. Ordinary partitioning schemes are summarised in the following subsections.

3.1 Interleaving Segmentation Scheme (IL-PTS)

Figure 2 depicts the IL-PTS algorithm, in which N/V subcarriers allocate equal V intervals within the subblocks. Thus, V-1 of zeros inside every subblock separates the active subcarriers. The PAPR reduction capacity of the IL-PTS is the worst among the three ordinary division schemes [24]. They are owing to the periodic pattern of the subcarriers in the IL-PTS structure, which imposes a high correlation among the subcarriers.

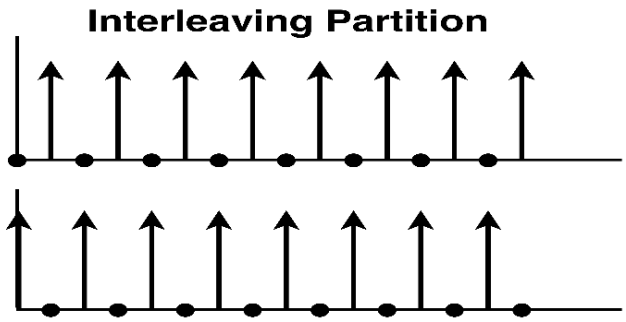

Figure 2. Interleaving segmentation scheme

By contrast, the CC of the IL-PTS method is reduced by applying the divide-and-conquer approach via Cooley–Tukey IFFT transformation. In every single subblock of the IL-PTS, the data vector is arranged column-wise, in which the number of subblocks equals the total number of rows V in the IL-PTS. Meanwhile, the number of subsets equals the number of columns R in one subblock, as shown in **Table 1**. However, the signal obtained from every subblock is restored via row-wise mapping based on the divide-and-conquer approach.

Table 1 Subblock arrangement of the IL-PTS method

$v \setminus r$	1	2	…	R
1	Y_1^v	Y_{V+1}^v	…	$Y_{V(R-1)+1}^v$
2	Y_2^v	Y_{V+2}^v	…	$Y_{V(R-1)+2}^v$
…	…	…	…	…
V	Y_V^v	Y_{2V}^v	…	Y_{VR}^v

The TD signal of the rows and columns in **Table 1** is expressed in **Eq. (11)** by utilising the Cooley–Tukey IFFT algorithm.

$$y_{(q,p)} = \frac{1}{N}\sum_{v=1}^{V}\left\{W_N^{vq}\left[\sum_{r=1}^{R} Y_{v,r}\, W_R^{rq}\right]\right\} W_V^{vq} \tag{11}$$

Where $W_N^{vq} = e^{j2\pi vq/N}$, $W_R^{rq} = e^{j2\pi rq/R}$, and $W_V^{vq} = e^{j2\pi vq/V}$ are the twiddle factors, while p and q, where $1 \le p \le V$ and $1 \le q \le R$ represent the elements of the p-th row and q-th column of y(q,p), respectively. The active subcarriers are located only at the v row depending on the IL property of the IL-PTS method; therefore, R-IFFT is performed only at the v row, and the formula above can be simplified as **Eq. (12)**.

$$y_{(q,p)} = \frac{1}{N} W_N^{v(Rp+q)} \sum_{r=1}^{R} Y_{v,r} W_R^{rq} \tag{12}$$

Thus, each subblock of the IL-PTS needs to compute only one R-IFFT and N-times complex multiplications. Therefore, the number of the addition (C_{add-IL}) and multiplication operations ($C_{mult-IL}$) of the IL-PTS is written as in **Eq. (13 and 14)** [23].

$$C_{add-IL} = V\left[\frac{N}{V}\, log_2 \frac{N}{V}\right] \tag{13}$$

$$C_{mult-IL} = V\left[\frac{N}{2V}\, log_2 \frac{N}{V} + N\right] \tag{14}$$

The CC of the IL-PTS is the lowest among the traditional schemes [24]. This result is because the IL-PTS method requires few IFFT stages to transform the subblocks in the TD depending on the Cooley–Tukey IFFT algorithm.

3.1.1. Pseudo-random Segmentation Scheme (PR-PTS)

The PR-PTS algorithm is the most convenient traditional segmentation scheme with PAPR reduction capacity [24]. In the PR-PTS, the subcarriers are allocated arbitrarily within the subblocks, with active subcarriers assigned only once inside each subblock, as shown in **Figure 3**.

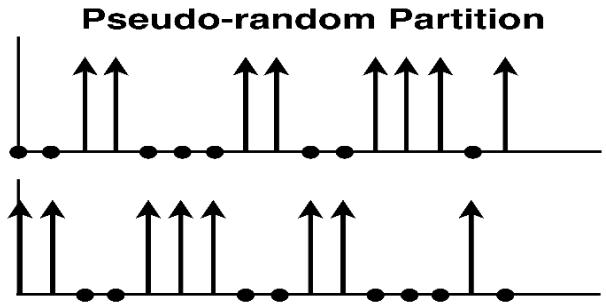

Figure. 3 Pseudo-random segmentation scheme

Figure 3 shows the PR-PTS scheme for two subblocks. The PR-PTS method can realise significant PAPR reduction, as it has low autocorrelation among the subcarriers inside the subblocks [25]. By contrast, high CC is considered as an inherent feature of the PR-PTS method, which can be assigned to the random distribution of the subcarriers. Thus, all the stages of the IFFT operation should be performed using the PR-PTS method when transforming the subblocks in the TD. The number of addition (C_{add-PR}) and multiplication operations (C_{add-PR}) of the PR-PTS method is written in **Eqs. (15) and (16)** utilising the Cooley–Tukey IFFT algorithm as:

$$C_{mult-PR} = V\left[\frac{N}{2} log_2 N\right] \quad (15)$$

$$C_{add-PR} = V[N log_2 N] \quad (16)$$

3.1.2. Adjacent Segmentation Scheme (Ad-PTS)

The Ad-PTS algorithm involves a simple partitioning process, but its PAPR reduction performance is lower than that of the PR-PTS scheme. N/V consecutive subcarriers are assigned sequentially inside the subblocks of the Ad-PTS, and the rest positions of the subblocks are set to zeros, as shown in **Figure 4**.

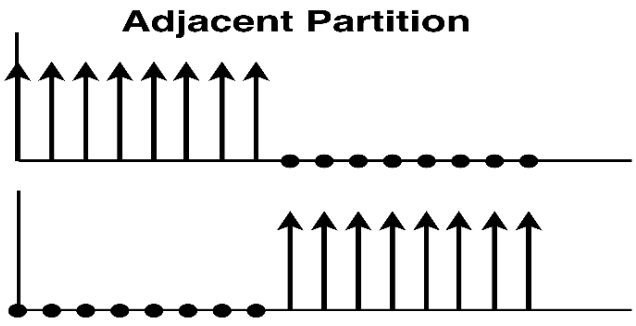

Figure. 4 Adjacent segmentation scheme

Accordingly, the CC of the Ad-PTS is similar to that of the PR-PTS [25] because the Ad-PTS performs all the IFFT stages to transform the subblocks in the TD. The number of addition (C_{add-Ad}) and multiplication operations ($C_{mult-Ad}$) of the Ad-PTS is expressed in **Eqs. (17) and (18)** by implementing the Cooley–Tukey IFFT algorithm as [23].

$$C_{add-Ad} = V[N\ log_2\ N] \tag{17}$$

$$C_{mult-Ad} = V\left[\frac{N}{2}\ log_2 N\right] \tag{18}$$

4. Proposing Algorithm (R-PTS)

In this section, a new segmentation method is proposed to enhance PAPR reduction capacity. In OFDM systems, the input data symbol has a noticeable correlation with its elements; thus, the transmitted OFDM signal will include a high PAPR value [25]. The proposing algorithm depends on the rotation of several subcarriers inside the subblocks arranged in a specific pattern to downgrade the correlation of the subcarriers. Hence, the PAPR value of the OFDM signal is reduced, accordingly. The procedure of the rotation PTS algorithm (R-PTS) begins when the input data sequence Y is divided into V subblocks similar to the partitioning operation of the traditional segmentation schemes, as given in **Eq. (5)**, which is rewritten below for convenience.

$$Y = \sum_{v=1}^{V} Y_v \tag{19}$$

Where Y_v is the partitioned subblocks. Subsequently, each subblock is subdivided into two equal parts, that is, Av and Bv,

$$Y_v = [A_v, B_v] \tag{20}$$

In which,

$$A_v = \left[Y_{v,1}, Y_{v,2}, \ldots \ldots, Y_{v,N/2}\right] \tag{21}$$

And,

$$B_v = \left[Y_{v,(N/2)+1}, Y_{v,(N/2)+2}, \ldots\ldots, Y_{v,N/2}\right] \tag{22}$$

Next, the first element is exchanged with the last element in each part of the subblocks. Therefore, the two parts of a subblock can be expressed as:

$$A_v^{'} = [Y_{v,N/2}, Y_{v,2}, \ldots\ldots, Y_{v,1}] \tag{23}$$

$$B_v^{'} = [Y_{v,N}, Y_{v,(N/2)+2}, \ldots\ldots, Y_{v,(N/2)+1} \tag{24}$$

The rotation process is implemented for all the subblocks in the PTS matrix. Therefore, the new matrix of the R-PTS method can be expressed as:

$$Y' = \sum_{v=1}^{V} Y'_v \tag{25}$$

In which,

$$Y'_v = [A_v^{'}, B_v^{'}] \tag{26}$$

Therefore, the final R-PTS matrix is,

$$Y' = \begin{bmatrix} Y_{1,N/2} & Y_{1,2} & \cdots & Y_{1,1} & Y_{1,N} & Y_{1,(N/2)+2} & \cdots & Y_{1,(N/2)+1} \\ Y_{2,N/2} & Y_{2,2} & \cdots & Y_{2,1} & Y_{2,N} & Y_{2,(N/2)+2} & \cdots & Y_{2,(N/2)+1} \\ \vdots & \vdots & \vdots & \vdots & \vdots & \vdots & \vdots & \vdots \\ Y_{v,N/2} & Y_{v,2} & \cdots & Y_{v,1} & Y_{v,N} & Y_{v,(N/2)+2} & \cdots & Y_{v,(N/2)+1} \end{bmatrix} \tag{27}$$

The R-PTS algorithm exchanges the terminal samples within the subblocks; thus, the correlation among the samples will be lower than that in the original matrix. Accordingly, the PAPR reduction gain of the PTS technique will be improved. In this study, the R-PTS algorithm is applied to the three conventional segmentation schemes, as shown in the following subsections.

4.1. Rotation IL-PTS Scheme

As discussed in Section 2, the PAPR performance of the IL-PTS is the worst among the ordinary schemes. In this section, the R-PTS algorithm is applied to the IL-PTS to enhance the PAPR gain. The new algorithm is called the R-IL-PTS, as we can see in **Figure 5**.

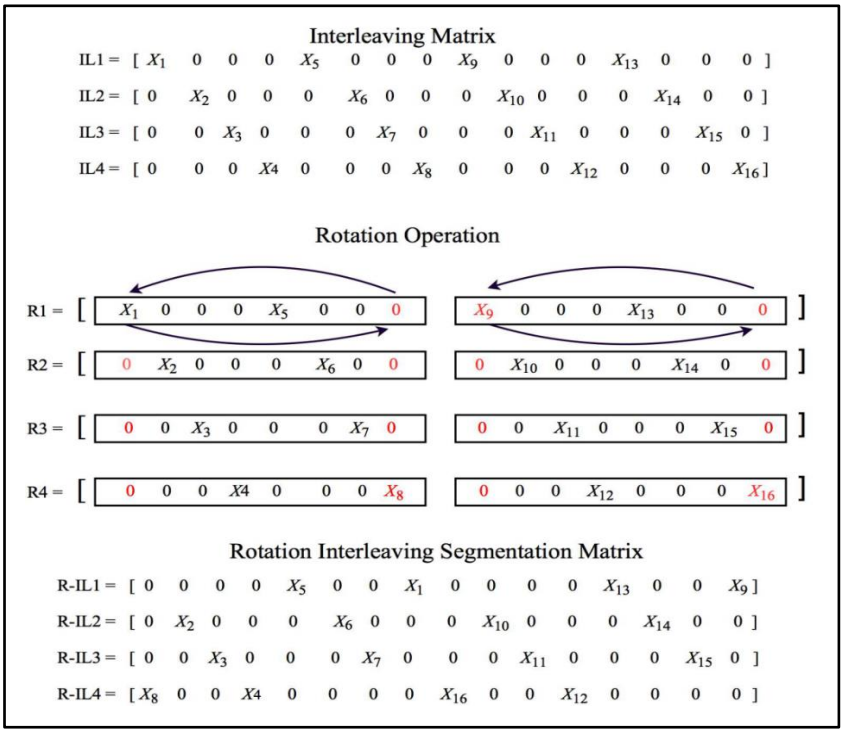

Figure. 5 R-IL-PTS segmentation scheme when N = 16 and V = 4

Figure 5 demonstrates the procedure of the R-IL-PTS algorithm, in which the V subblocks are extracted from the input data symbol like the IL-PTS scheme, and every subblock is subdivided into two parts. Next, in each part, the first sample is exchanged with the last sample, and this process continues until the last subblock obtains the final R-IL-PTS matrix. Finally, the R-IL-PTS algorithm is applied to the PTS procedure to produce the optimum OFDM signal. The PAPR reduction capacity of the R-IL-PTS is preferable to that of the IL-PTS and better than that of the Ad-PTS method. However, the CC of the R-IL-PTS algorithm in **Figure 5** is calculated using the divide-and-conquer approach with the Cooley–Tukey algorithm as well as the subblock arrangement in Table 1, where half of the subblocks in the R-IL-PTS algorithm are needed to compute two R-IFFT functions and N-times complex multiplications. The rest of the subblocks need to compute only one R-IFFT function and N-times complex multiplications. Therefore, the number of complex additions ($C_{add-R-IL}$) and complex multiplications ($C_{multi-R-IL}$) of the IL-PTS can be expressed in **Eqs. (28 and 29)** as follows:

$$C_{add-R-IL} = \frac{3N}{2} log_2\left(\frac{N}{V}\right) + N \tag{28}$$

$$C_{mult-R-IL} = \frac{3N}{4} log_2\left(\frac{N}{V}\right) + \frac{N}{2} + NV \tag{29}$$

4.2. Rotation Ad-PTS Scheme

As mentioned previously, the Ad-PTS algorithm is deemed the most straightforward implementation among the segmentation methods. The PAPR reduction capability of the Ad-PTS method is better than that of the IL-PTS but worse than that of the PR-PTS. In this section, the R-PTS algorithm is utilised with the Ad-PTS (R-Ad-PTS) to enhance PAPR reduction performance as can show in **Figure 6**.

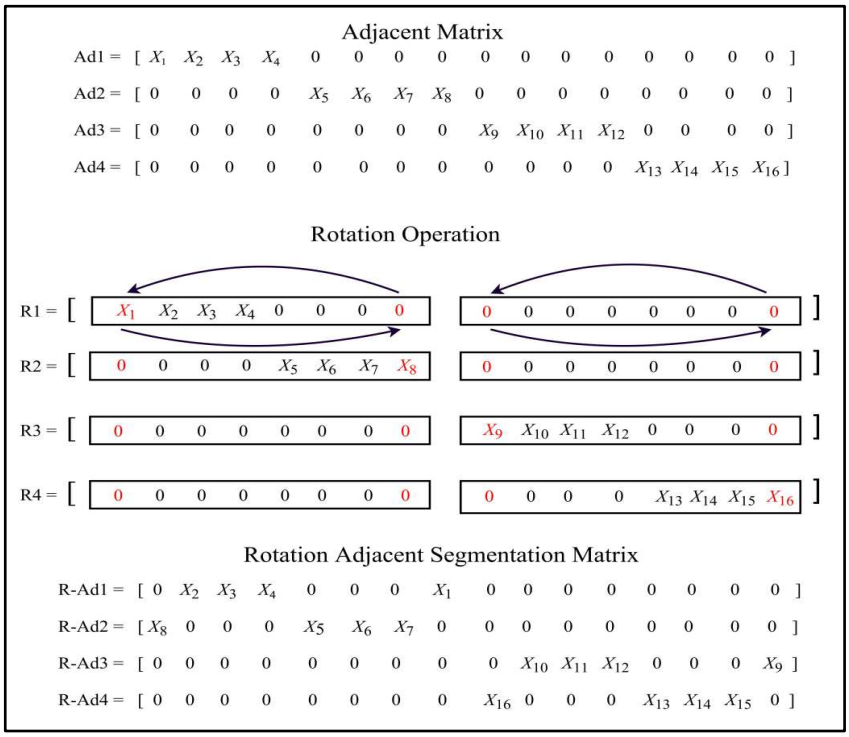

Figure. 6 R-Ad-PTS segmentation method, N = 16 and V=4

The input data symbol in **Figure 6** is segmented into V subblocks, which is like the procedure discussed for the Ad-PTS algorithm, and each subblock of the adjacent matrix is separated into two parts. However, in the subblocks, the samples of each part are modified by exchanging the first sample with the last sample. Lastly, the R-Ad-PTS matrix performs the remaining procedure of the PTS algorithm to produce the optimum OFDM signal.

The PAPR reduction performance of the R-Ad-PTS corresponds to that of the Ad-PTS algorithm because the correlation among the samples of the R-Ad-PTS is less than that among the samples of the Ad-PTS. However, CC is obtained according to the divide-and-conquer approach with the Cooley–Tukey algorithm and the subblock arrangement in **Table 1**, where each subblock in the R-Ad-PTS needs to compute three R-IFFT functions and N-

times complex multiplications. Accordingly, the number of the addition and multiplication complexities of the R-Ad-PTS is obtained as **Eqs. (30 and 31)**.

$$C_{add-R-Ad} = 3N\left[log_2\left(\frac{N}{V}\right) + log_2 3\right] \tag{30}$$

$$C_{mult-R-Ad} = \frac{3N}{2}\left[log_2\left(\frac{N}{V}\right) + log_2 3\right] + NV \tag{31}$$

4.3. Rotation PR-PTS Scheme

In this study, we classify the PR-PTS as the best partitioning scheme among the ordinary segmentation methods in terms of PAPR reduction efficiency. Sample exchange is applied to the R-PR-PTS to lessen the PAPR pattern. The procedure of the R-PR-PTS is the same as that of the Ad-PTS and IL-PTS, except the input data symbol is partitioned similar to the PR-PTS, as demonstrated in **Figure 7**. The PAPR-reducing capability of the R-PR-PTS method is similar to that of the PR-PTS algorithm, as illustrated in the next section. This similarity is because the random property of the PR-PTS matrix can achieve the lowest subcarrier correlation inside the subblocks. Therefore, the PAPR-reducing efficiency of the R-PR-PTS is uninfluenced by the rotation algorithm. By contrast, the CC of the R-PR-PTS algorithm is the same as that of the PR-PTS, as the subcarriers are allocated randomly inside each subblock. Thus, all the stages of the IFFT operation must be performed when transforming the subblocks in the TD.

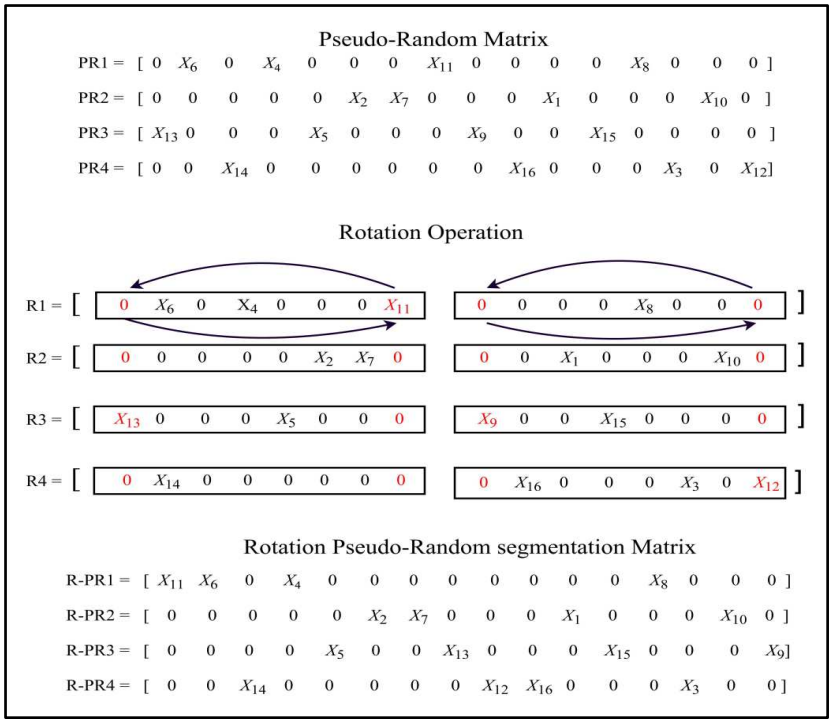

Figure. 7 PR-PTS segmentation method, N = 16 and V = 4

4. Results and Discussion

4.1. Simulation Results Analysis

The PAPR reduction performance of the standard and enhanced algorithms is analysed. In terms of the parameters utilised in the simulation, the subblock number V is 4, the subcarrier numbers N are 128 and 256, the oversampling factor L equals 4 and the number of the different phase coefficient vectors W is 4. The CCDF is employed to evaluate the PAPR pattern of the input symbols, and 16-QAM is adopted for constellation mapping. Firstly, simulation is conducted to evaluate the three ordinary segmentation schemes, as shown in **Figures 8 and 9**. In case the number of subcarriers is 128, the PAPR value of the PR-PTS is 7.11 dB, that of the IL-PTS is 8.24 dB, and that of the original signal (without a reduction technique) is 10.79 dB, as shown in **Figure 8.** Furthermore, when N = 256, the PAPR capacity of the PR-PTS, Ad-PTS, IL-PTS and original OFDM is 7.68dB, 8.24 dB, 8.52 dB and 11.07 dB, respectively, as shown in **Figure 9**. As a result, the PR-PTS algorithm is the best segmentation scheme, whereas the Ad-PTS algorithm demonstrates a lower reduction performance compared with the PR-PTS. By contrast, the IL-PTS algorithm is the worst segmentation scheme in terms of PAPR reduction efficiency.

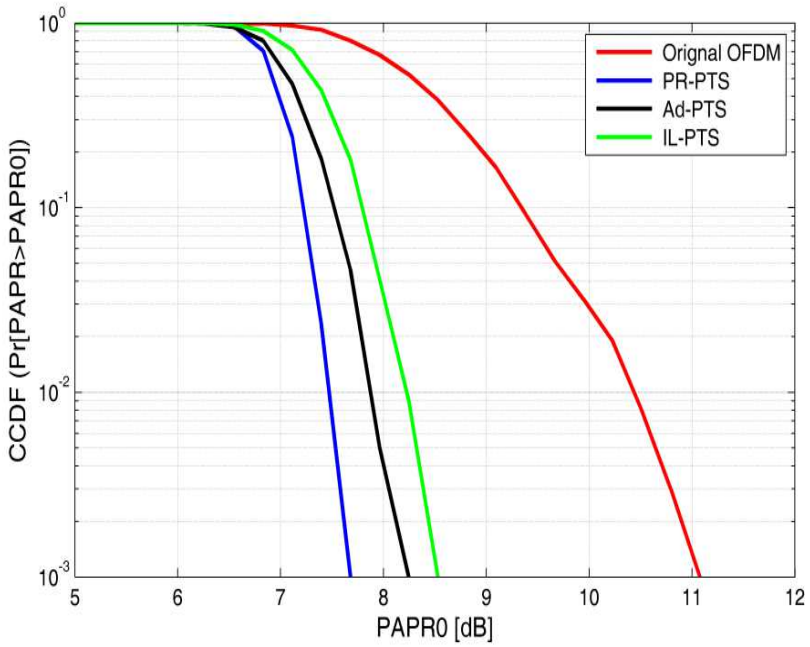

Figure. 8 Comparison of the three ordinary partitioning methods, N =128 and V= 4

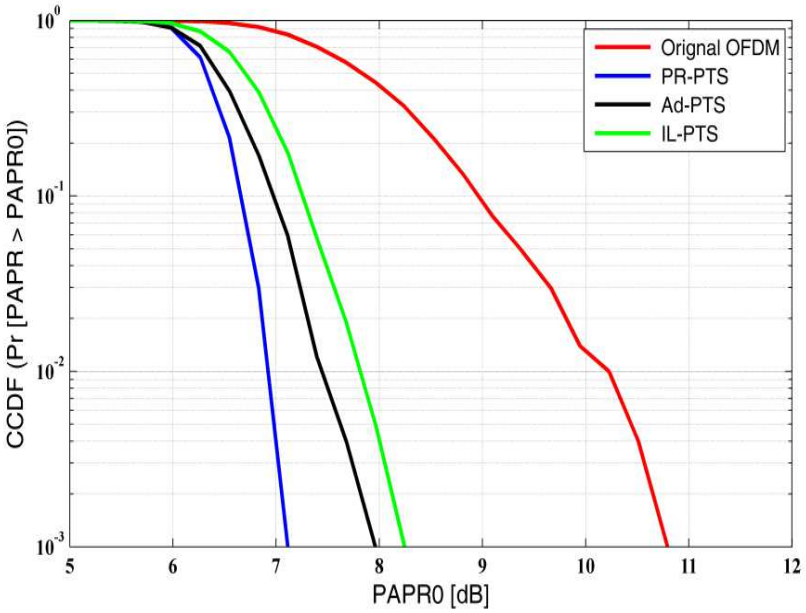

Figure. 9 Comparison of the three ordinary partitioning methods, N = 256 and V=4

Figures 10 and 11 compare the R-IL-PTS algorithm with the Ad-PTS and IL-PTS ordinary segmentation methods when N = 128 and 256. In the first scenario, when N is set to 128, the R-IL-PTS method outperforms the original signal by 2.88 dB, the Ad-PTS by 0.28 dB and the IL-PTS by 0.56 dB, as depicted in **Figure 10**. However, in the second scenario, when N = 256, the R-IL-PTS outperforms the original OFDM by 3.46 dB and the IL-PTS. By 0.28 dB. Meanwhile, the R-IL-PTS and Ad-PTS achieve the same PAPR performance at 8.24 dB, as demonstrated in **Figure 11**. Therefore, the PAPR reduction capacity of the proposed method, that is, the R-IL-PTS, is better than that of the IL-PTS and the same as that of the Ad-PTS.

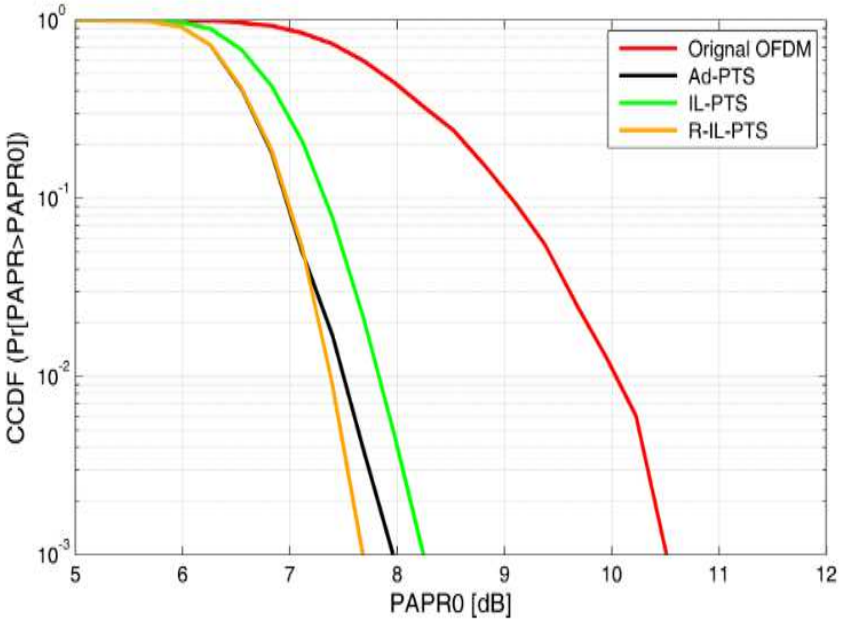

306

307 Figure 10. Comparison R-IL-PTS, IL-PTS and Ad-PTS, N = 128 and V= 4

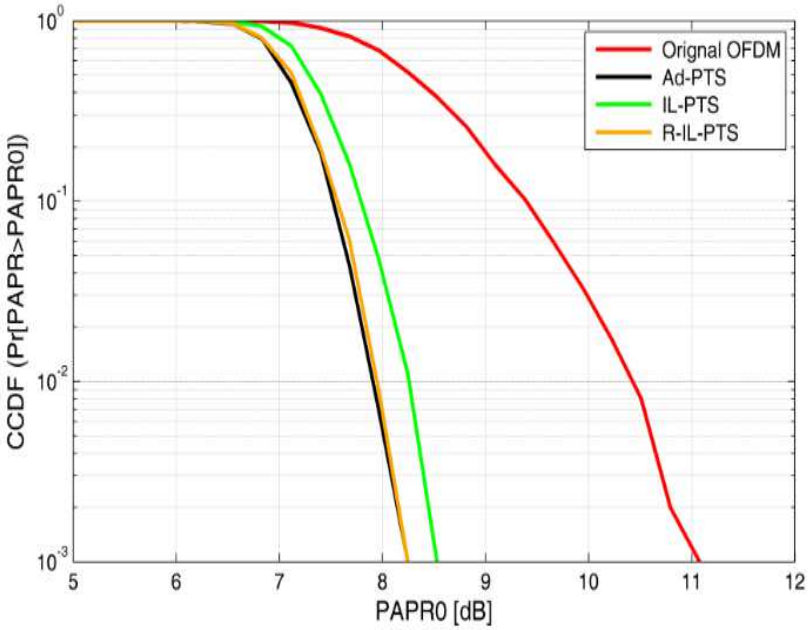

308

309 Figure 11. Comparison R-IL-PTS, IL-PTS and Ad-PTS, N = 256 and V= 4

310 In the simulation results shown in **Figures 12 and 13**, the PAPR reduction efficiency of the R-Ad-PTS
311 is compared with that of the Ad-PTS, IL-PTS and OFDM signal when N = 128 and 256. In **Figure 12**, when N =
312 128, the R-Ad-PTS algorithm outperforms the Ad-PTS, IL-PTS and original OFDM by 0.57 dB, 0.85 dB and 3.4
313 dB, respectively. However, when N is set to 256, the R-Ad-PTS algorithm exceeds the Ad-PTS by 0.28 dB, the

IL-PTS by 0.56 dB and the original OFDM by 3.74 dB, as shown in **Figure 13**. Consequently, the enhanced R-Ad-PTS algorithm can reduce PAPR values better than the Ad-PTS for any number of subcarriers.

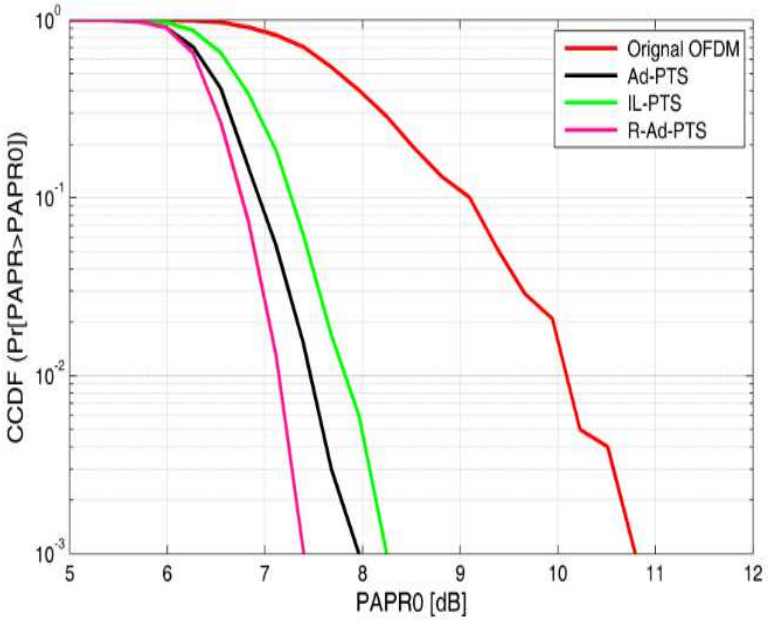

Figure 12. Comparison R-Ad-PTS, Ad-PTS and IL-PTS, N = 128 and V= 4

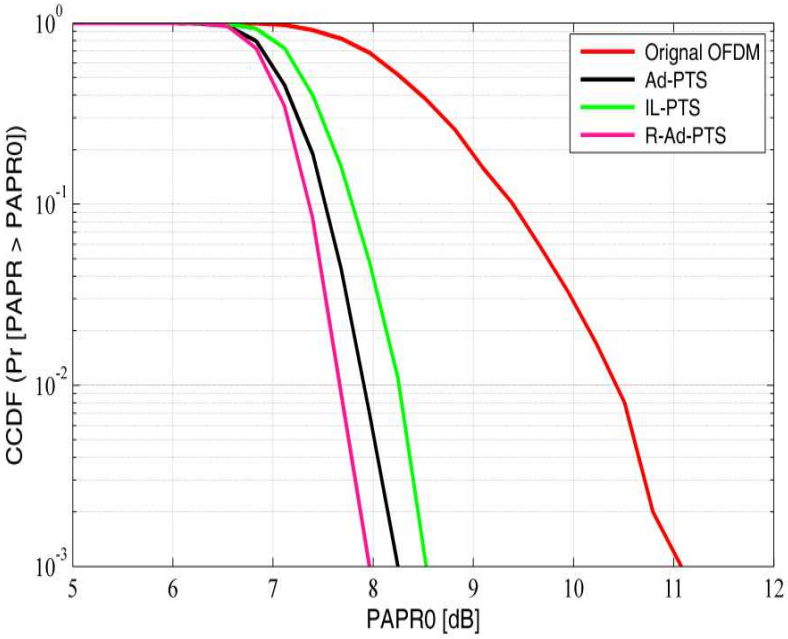

Figure 13. Comparison R-Ad-PTS, Ad-PTS and IL-PTS, N = 256 and V= 4

Moreover, the simulation results in **Figure 14 and 15** illustrate the influence of the R-PR-PTS on PAPR reduction capacity. When N is set to 128, the PAPR level of the R-PR-PTS is 6.95 dB, whereas that of the PR-

PTS and the ordinary signal is 7.12 dB and 10.78dB, as shown in **Figure 14**. However, when N is set to 256, the PAPR value of the R-PR-PTS reaches 7.6 dB, whereas that of the PR-PTS and original OFDM is 7.72dB and 10.91 dB, respectively, as presented in **Figure 15**. Moreover, the proposed R-PR-PTS method has a slight influence on PAPR reduction capacity compared with the PR-PTS, because the R-PR-PTS and P-PTS have nearly the same effect on the correlation of the subcarriers within the subblocks.

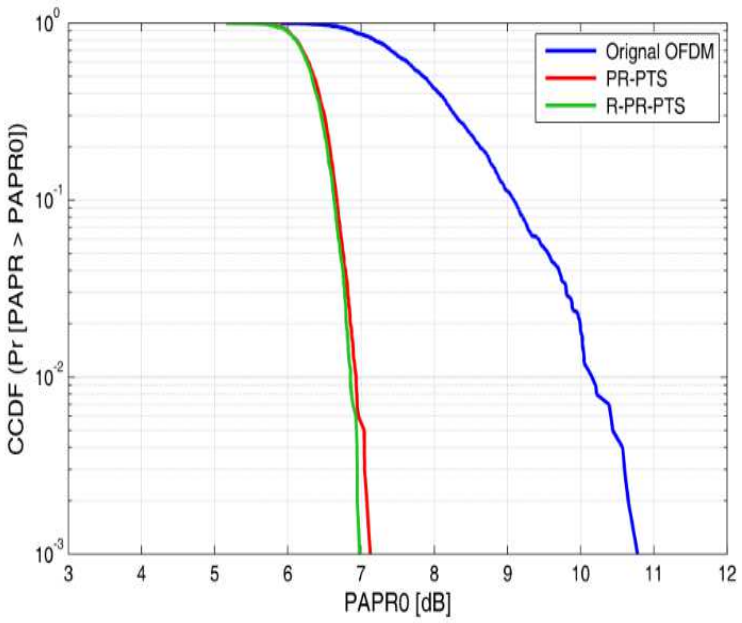

Figure 14. Comparison R-PR-PTS and PR-PTS, N = 128 and V= 4

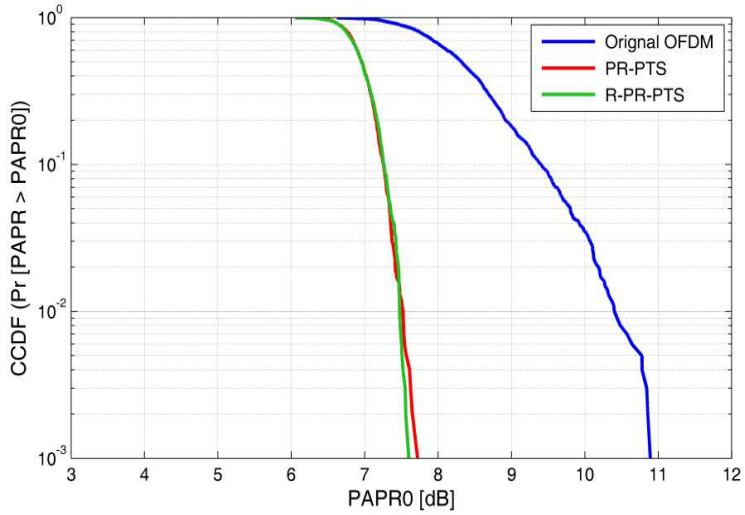

Figure 15. Comparison R-PR-PTS and PR-PTS, N = 256 and V= 4

4.4. Numerical Results Analysis

From the perspective of mathematical calculations, the proposed method demonstrates different CC levels when the three traditional segmentation schemes are applied. **Tables 2 and 3** record the CC level of the ordinary and improved partitioning schemes, namely, the R-IL-PTS, R-Ad-PTS and R-PR-PTS, as well as the calculations of the CC reduction ratio (CCRR) of the different simulated schemes, where the CCRR between the proposed and corresponding traditional schemes can be expressed as [26] in **Eq. (32)** below.

$$\mathrm{CCRR} = 1 - \frac{Complexity\ of\ proposed\ scheme}{complexity\ of\ conventional\ scheme} \times 100\% \tag{32}$$

Table 2 CCRR of the traditional and the improved schemes when N= 128

N= 128, V= 4				
PTS method	C_{add}	C_{mult}	$CCRR_{add}$	$CCRR_{mult}$
IL-PTS	640	832	-41.17%	-21.21%
R-IL-PTS	1088	1056		
Ad-PTS	3584	1792	29.44%	1.05%
R-Ad-PTS	2528.64	1776.32		
PR-PTS	3584	1792	0%	0%
R-PR-PTS	3584	1792		

Table 3 CCRR of the traditional and the improved schemes when N= 256

N= 256, *V*= 4				
PTS method	C_{add}	C_{mult}	$CCRR_{add}$	$CCRR_{mult}$
IL-PTS	1536	1792	-40%	-22.22%
R-IL-PTS	2560	2304		
Ad-PTS	8192	4096	28.9%	3.9%
R-Ad-PTS	5825.28	3936.64		
PR-PTS	8192	4096	0%	0%
R-PR-PTS	8192	4096		

In Tables 2 and 3, when the R-PTS algorithm is applied to the IL-PTS, the number of complex addition and multiplication operations is higher than that in the IL-PTS for both scenarios (N = 128 and 256). Therefore, when N =128, improvement of PAPR performance when the proposed algorithm is applied to the IL-PTS is at the expense of degradation in the CCRRadd and CCRRmult, where CCRRadd increases by 41.17%, and CCRRmult

increases by 21.21. Similarly, when N = 256, the CCRRadd of the R-IL-PTS algorithm records degradation by 40%, whereas the CCRRmult records degradation by 22.22%. Furthermore, when N = 128, CCRRadd and CCRRmult are increased to 29.44% and 1.05%, respectively, when the R-PTS algorithm is applied to the Ad-PTS scheme. Likewise, when the number of subcarriers equals 256, CCRRadd and CCRRmult are increased by 28.9% and 3.9%, respectively. Accordingly, the proposed method improves the Ad-PTS scheme in terms of PAPR reduction performance and CC level. Finally, the CC level of the R-PR-PTS and PR-PTS schemes is the same for both scenarios. This result can be referred to the fact that the random nature of these schemes makes the subblocks perform all the IFFT stages when transforming the data in the TD.

5. Conclusion

A new algorithm for subblock segmentation in the PTS technique is proposed to restrain high PAPR values in OFDM systems. The conducted algorithm relies on dividing every subblock of the PTS technique into two parts and exchanging the first and last samples in each part to obtain a new segmentation scheme, which is called the R-PTS. The presented algorithm is analysed and applied to the conventional segmentation schemes. The results of the simulation indicate that the enhanced schemes, that is, R-IL-PTS and R-Ad-PTS, can accomplish PAPR reduction better than the corresponding ordinary schemes, that is, IL-PTS and Ad-PTS. However, the mathematical calculation model states that the CC level of the R-IL-PTS is higher than that of the IL-PTS, whereas the number of the process complexity for the R-Ad-PTS algorithm is lower than that for the Ad-PTS. However, the R-PR-PTS approach and PR-PTS scheme demonstrate the same PAPR reduction efficiency and CC level. Consequently, the rotation algorithm can be utilised as an effective method to achieve a high PAPR pattern with a low complexity level for the Ad-PTS scheme.

REFERENCES

1. Attiah, M. L., Isa, A. A. M., Zakaria, Z., Abdulhameed, M. K., Mohsen, M. K., & Ali, I. (2020). A survey of mmWave user association mechanisms and spectrum sharing approaches: an overview, open issues and challenges, future research trends. *Wireless Networks*, *26*, 2487–2514. https://doi.org/10.1007/s11276-019-01976-x
2. Attiah, M. L., Isa, A. A. M., Zakaria, Z., Mohsen, M. K., Abdulhameed, M. K., & Dinar, A. M. (2020). Joint QoE-based user association and efficient cell–carrier distribution for enabling fully hybrid spectrum sharing approach in 5G mmWave cellular networks. *Wireless Networks*, *26*, 2487–2514. https://doi.org/10.1007/s11276-019-02109-0

3. Padarti, V. K., & Rao, N. V. (2020). Adaptive SOICAF Algorithm for PAPR Mitigation in OFDM Systems. *Wireless Personal Communications*, *113*(2), 927–943. https://doi.org/10.1007/s11277-020-07260-y

4. Jawhar, Y. A., Audah, L., Taher, M. A., Ramli, K. N., Shah, N. S. M., Musa, M., & Ahmed, M. S. (2019). A Review of Partial Transmit Sequence for PAPR Reduction in the OFDM Systems. *IEEE Access*, *7*, 18021–18041. https://doi.org/10.1109/ACCESS.2019.2894527

5. Ibraheem, Z. T., Rahman, M. M., Yaakob, S. N., Razalli, M. S., & Kadhim, R. A. (2015). Effect of partition length variability on the performance of adjacent partitioing PTS in papr reduction of OFDM systems. *ISCAIE 2014 - 2014 IEEE Symposium on Computer Applications and Industrial Electronics*, 24–28. https://doi.org/10.1109/ISCAIE.2014.7010203

6. Vidya, M., Vijayalakshmi, M., & Ramalingareddy, K. (2016). Performance enhancement of efficient partitioning technique for PAPR reduction in MIMO-OFDM system using PTS. *2015 Conference on Power, Control, Communication and Computational Technologies for Sustainable Growth, PCCCTSG 2015*, 247–253. https://doi.org/10.1109/PCCCTSG.2015.7503942

7. Wen, Q., Xiao, Y., & Li, S. (2007). Improved PTS for PAPR Reduction in OFDM Systems. *ICCCAS 2007 - International Conference on Communications, Circuits and Systems 2007*, 280–283. https://doi.org/10.1109/ICCCAS.2007.6250053

8. Hong, C., Qin, Q., & Chao, T. (2013). An PTS optimization algorithm for PAPR reduction of OFDM system. *Proceedings - 2013 International Conference on Mechatronic Sciences, Electric Engineering and Computer, MEC 2013*, 3775–3778. https://doi.org/10.1109/MEC.2013.6885649

9. Miao, L., & Sun, Z. (2013). PTS algorithm for PAPR suppression of WOFDM system. *Proceedings - 2013 International Conference on Mechatronic Sciences, Electric Engineering and Computer, MEC 2013*, (3), 1144–1147. https://doi.org/10.1109/MEC.2013.6885236

10. Taher, M. A., Radhi, H. S., & Jameil, A. K. (2020). Enhanced F-OFDM candidate for 5G applications. *Journal of Ambient Intelligence and Humanized Computing*, (0123456789). https://doi.org/10.1007/s12652-020-02046-3

11. León, O., Hernández-Serrano, J., & Soriano, M. (2010). Securing cognitive radio networks. *International Journal of Communication Systems*, *23*(5), 633–652. https://doi.org/10.1002/dac

12. Taher, M. A., Mandeep, J. S., Ismail, M., Samad, S. A., & Islam, M. T. (2010). Reducing the power envelope fluctuation of OFDM systems using side information supported amplitude clipping approach. *International Journal of Circuit Theory and Applications*, *24*(4), 425–435. https://doi.org/10.1002/cta

13. Taher, M. A., Mandeep, J. S., Ismail, M., Samad, S. A., & Islam, M. T. (2013). Sliding the SLM-technique to reduce the non-linear distortion in OFDM systems. *Elektronika ir Elektrotechnika*, *19*(5), 103–111. https://doi.org/10.5755/j01.eee.19.5.2075

14. Jiang, T., & Wu, Y. (2008). An overview: Peak-to-average power ratio reduction techniques for OFDM signals. *IEEE Transactions on Broadcasting*, *54*(2), 257–268. https://doi.org/10.1109/TBC.2008.915770

15. Mueller, S. H., & Huber, J. B. (1997). Novel peak power reduction scheme for OFDM. *IEEE International Symposium on Personal, Indoor and Mobile Radio Communications, PIMRC*, *3*, 1090–1094. https://doi.org/10.1109/pimrc.1997.627054

16. Kim, K. H. (2016). On the shift value set of cyclic shifted sequences for PAPR reduction in OFDM systems. *IEEE Transactions on Broadcasting*, *62*(2), 496–500. https://doi.org/10.1109/TBC.2016.2529292

17. Mhatre, K., & Khot, U. P. (2015). Efficient Selective Mapping PAPR reduction technique. *Procedia Computer Science*, *45*, 620–627. https://doi.org/10.1016/j.procs.2015.03.117

18. Sundararajan, M., & Govindaswamy, U. (2014). Multicarrier spread spectrum modulation schemes and efficient FFT algorithms for cognitive radio systems. *Electronics* , *3*(3), 419–443. https://doi.org/10.3390/electronics3030419

19. Lee, K. S., Cho, Y. J., Woo, J. Y., No, J. S., & Shin, D. J. (2016). Low-complexity PTS schemes using OFDM signal rotation and pre-exclusion of phase rotating vectors. *IET Communications*, *10*(5), 540–547. https://doi.org/10.1049/iet-com.2015.0192

20. Joo, H. S., Kim, K. H., No, J. S., & Shin, D. J. (2017). New PTS Schemes for PAPR Reduction of OFDM Signals Without Side Information. *IEEE Transactions on Broadcasting*, *63*(3), 562–570. https://doi.org/10.1109/TBC.2017.2711141

21. Al-Jawhar, Y. A., Ramli, K. N., Taher, M. A., Shah, N. S. M., Audah, L., & Ahmed, M. S. (2018). Zero-padding techniques in OFDM systems. *International Journal on Electrical Engineering and Informatics*, *10*(4), 704–725. https://doi.org/10.15676/ijeei.2018.10.4.6

22. Tokur Bozkurt, Y., & Taşpınar, N. (2017). Peak-to-Average Power Ratio Reduction in Lifting Based Wavelet Packet Modulation Systems Using Differential Evolution Algorithm. *Wireless Personal Communications*, *94*(3), 1073–1086. https://doi.org/10.1007/s11277-016-3670-5

23. Park, D. C., & Kim, S. C. (2018). Partial Transmit Sequence Scheme for Envelope Fluctuation Reduction in OFDMA Uplink Systems. *IEEE Communications Letters*, *22*(8), 1652–1655. https://doi.org/10.1109/LCOMM.2018.2840542

24. Al-Jawhar, Y. A., Ramli, K. N., Taher, M. A., Audah, L., Shah, N. S. M., Ahmed, M. S., & Hammoodi, A. T. (2018). An enhanced partial transmit sequence based on combining hadamard matrix and partitioning schemes in OFDM systems. *International Journal of Integrated Engineering*, *10*(3), 1–7. https://doi.org/10.30880/ijie.2018.10.03.001

25. Hung, H. L. (2011). Using evolutionary computation technique for trade-off between performance peak-to average power ration reduction and computational complexity in OFDM systems. *Computers and Electrical Engineering*, *37*(1), 57–70. https://doi.org/10.1016/j.compeleceng.2010.08.002

26. Varahram, P., & Ali, B. M. (2011). A low complexity partial transmit sequence for peak to average power ratio reduction in OFDM systems. *Radioengineering*, *20*(3), 677–682.

Figures

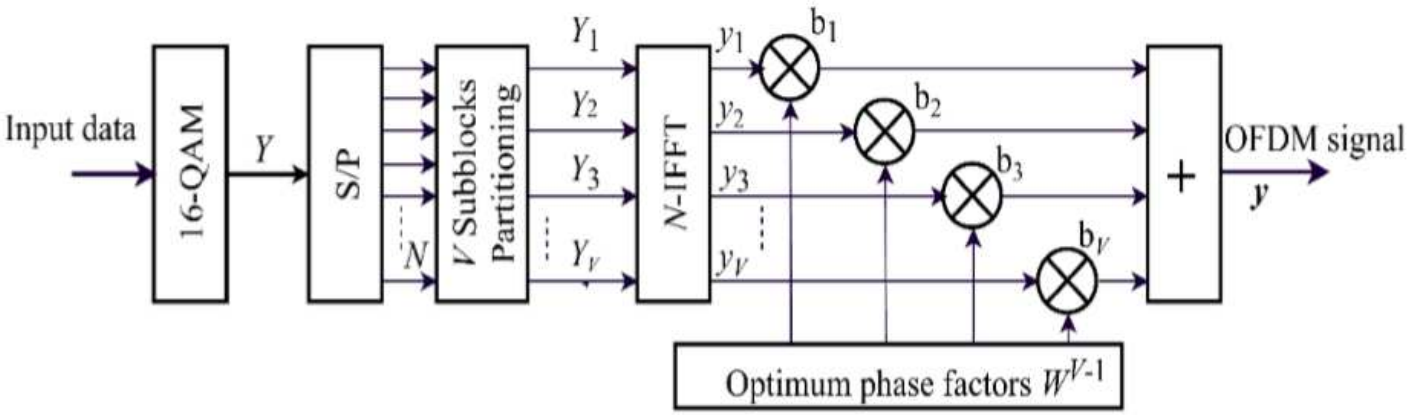

Figure 1

C-PTS block diagram [21]

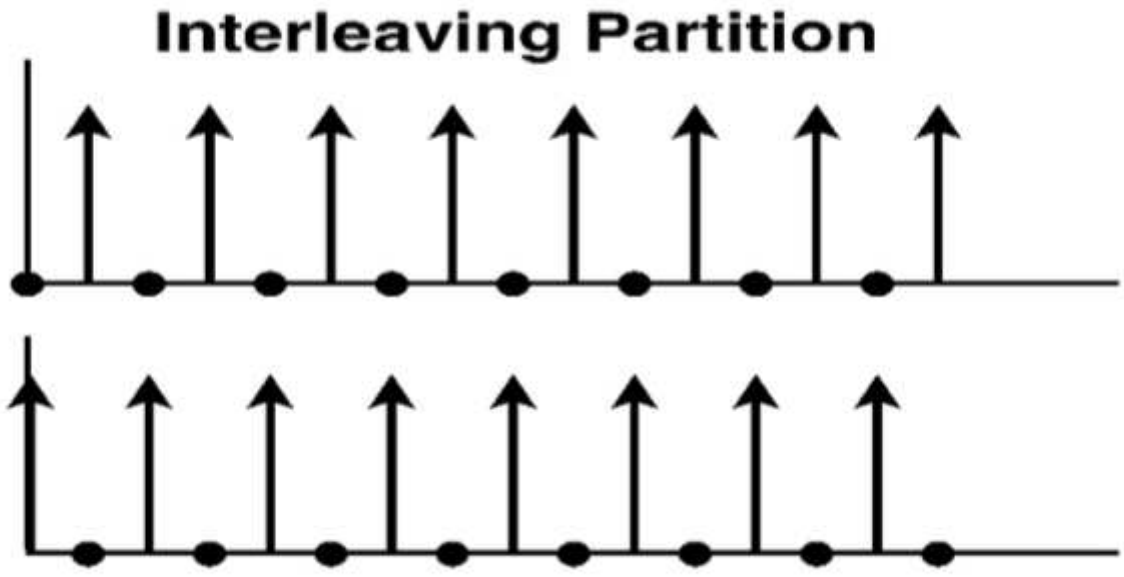

Figure 2

Interleaving segmentation scheme

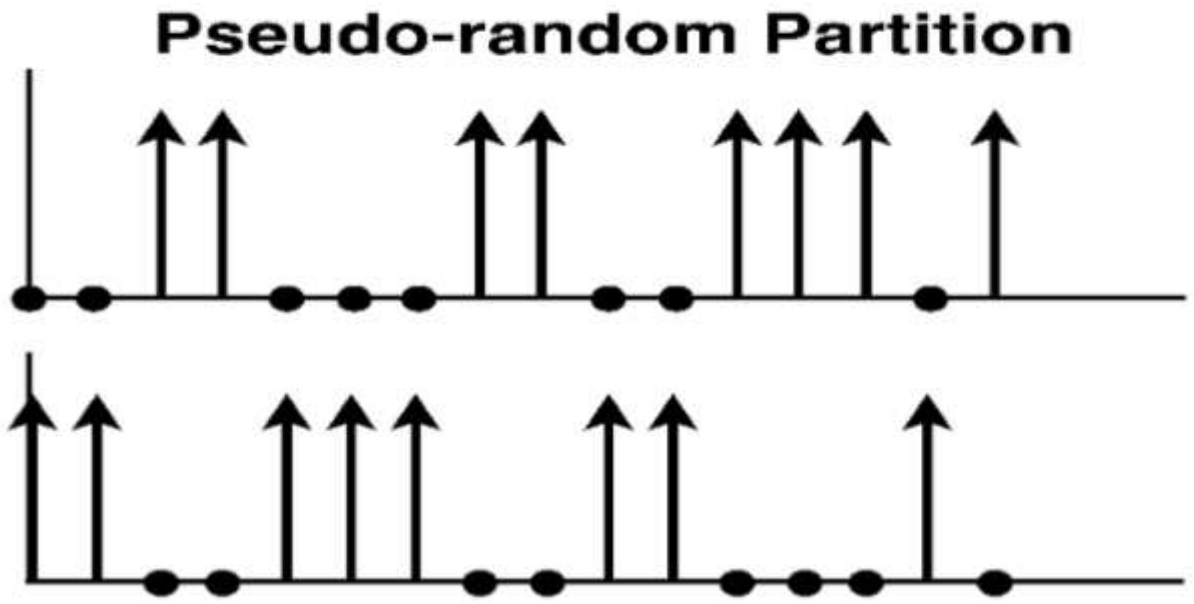

Figure 3

Pseudo-random segmentation scheme

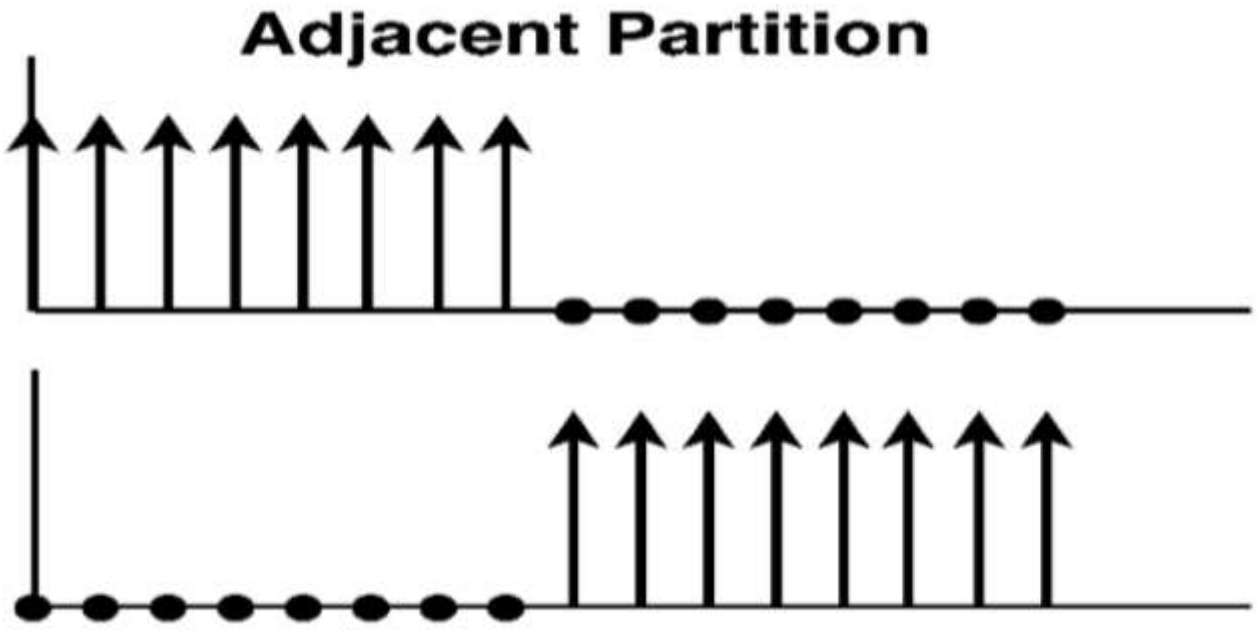

Figure 4

Adjacent segmentation scheme

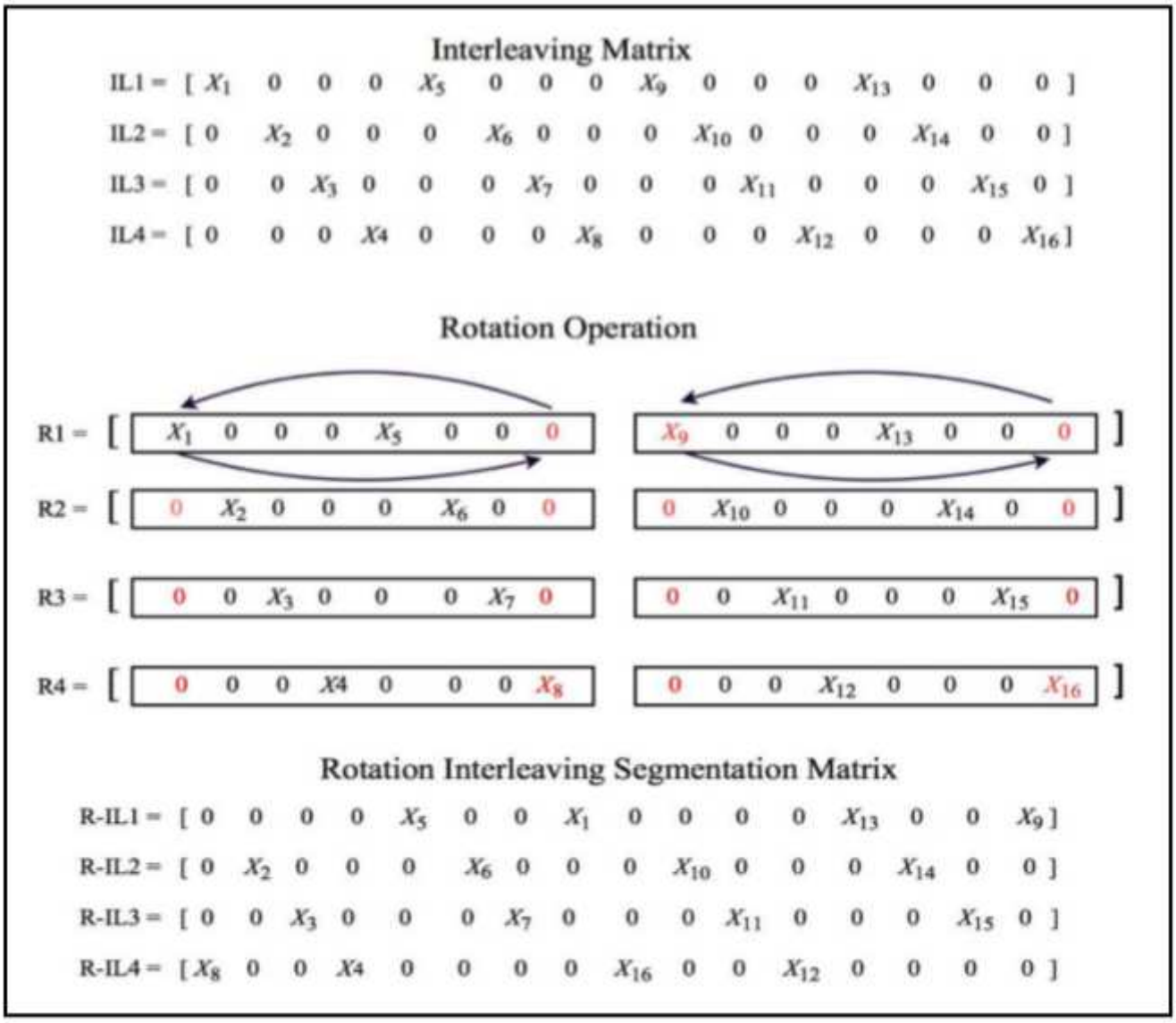

Figure 5

R-IL-PTS segmentation scheme when N = 16 and V = 4

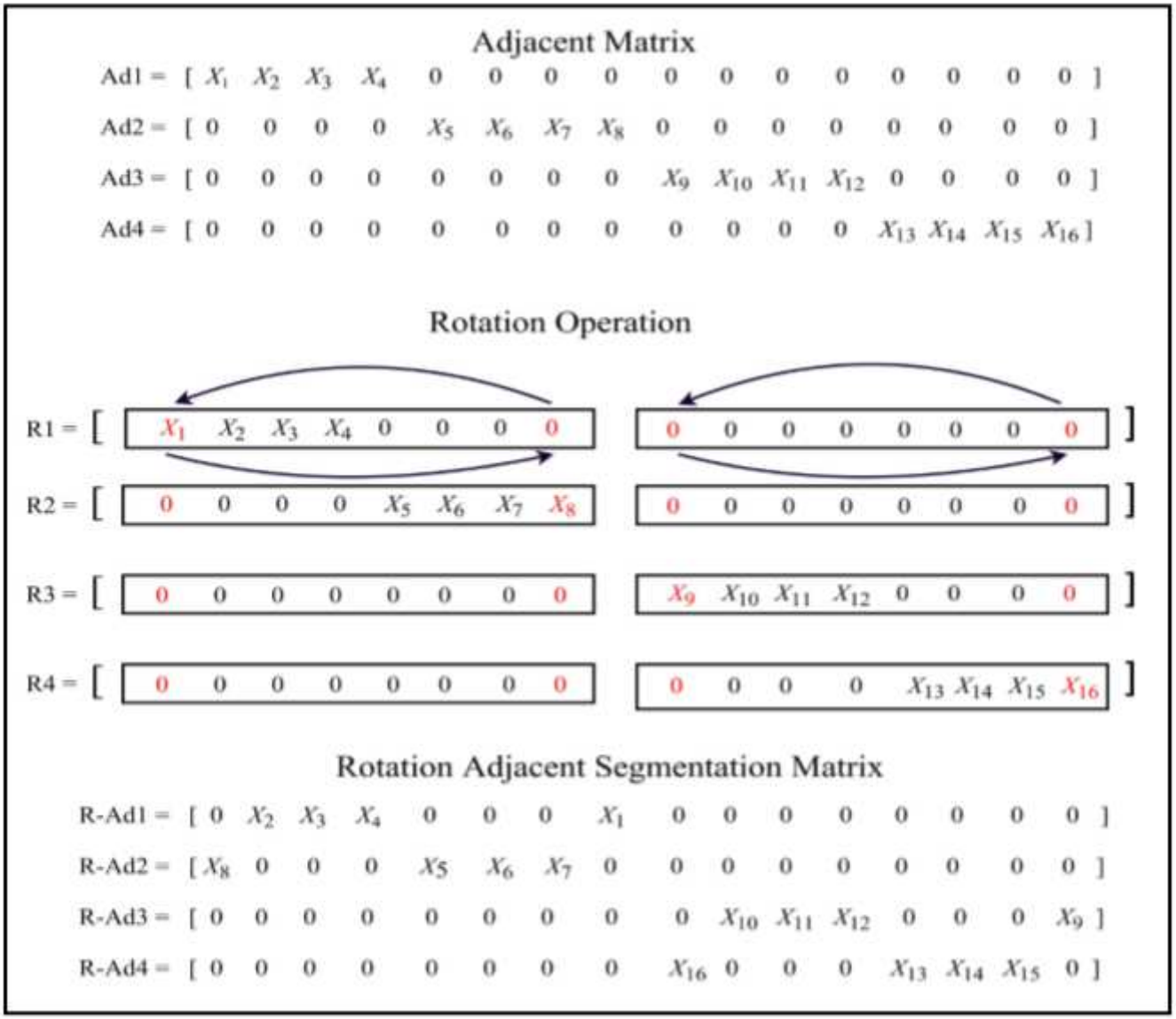

Figure 6

R-Ad-PTS segmentation method, N = 16 and V=4

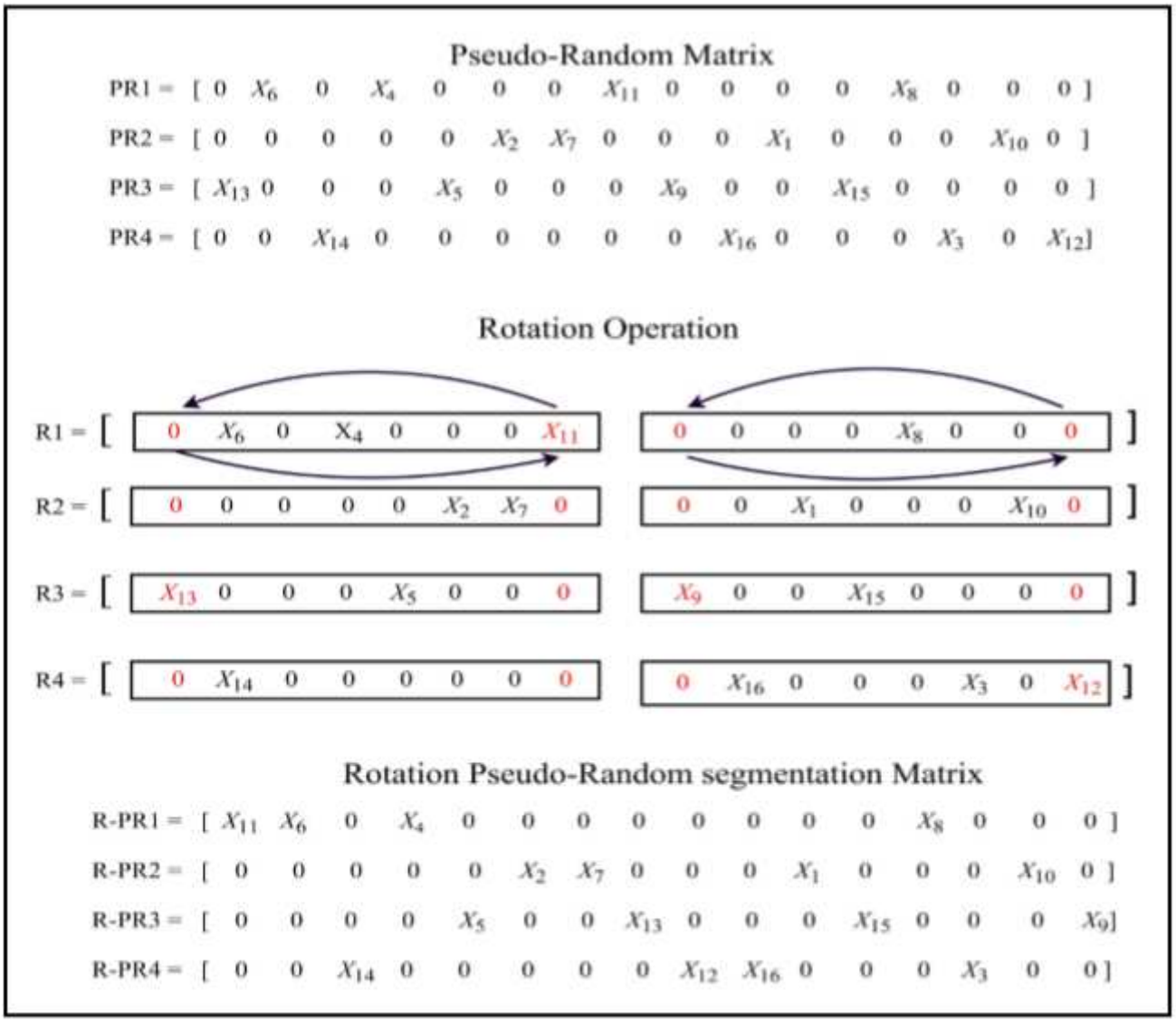

Figure 7

PR-PTS segmentation method, N = 16 and V = 4

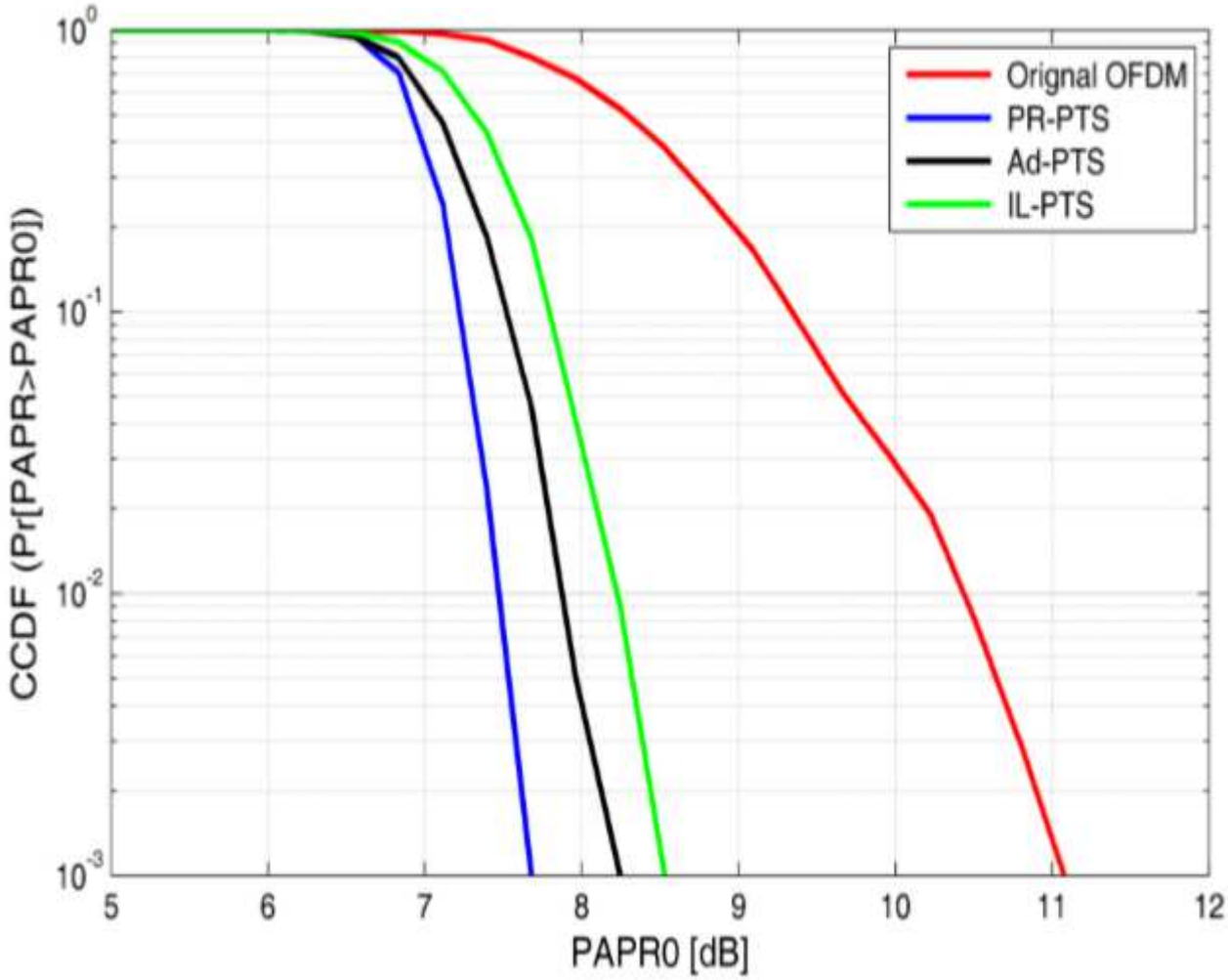

Figure 8

Comparison of the three ordinary partitioning methods, N =128 and V= 4

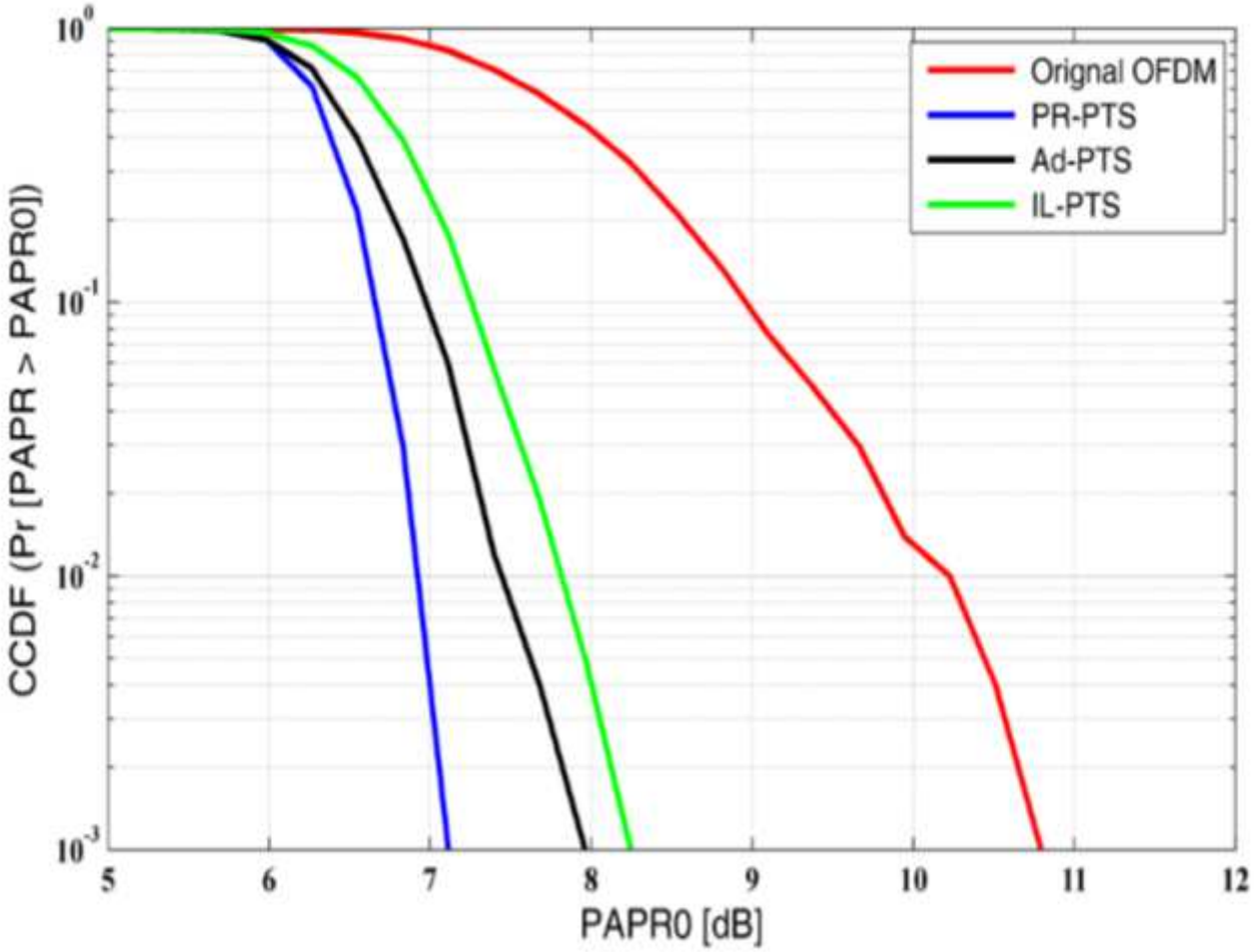

Figure 9

Comparison of the three ordinary partitioning methods, N = 256 and V=4

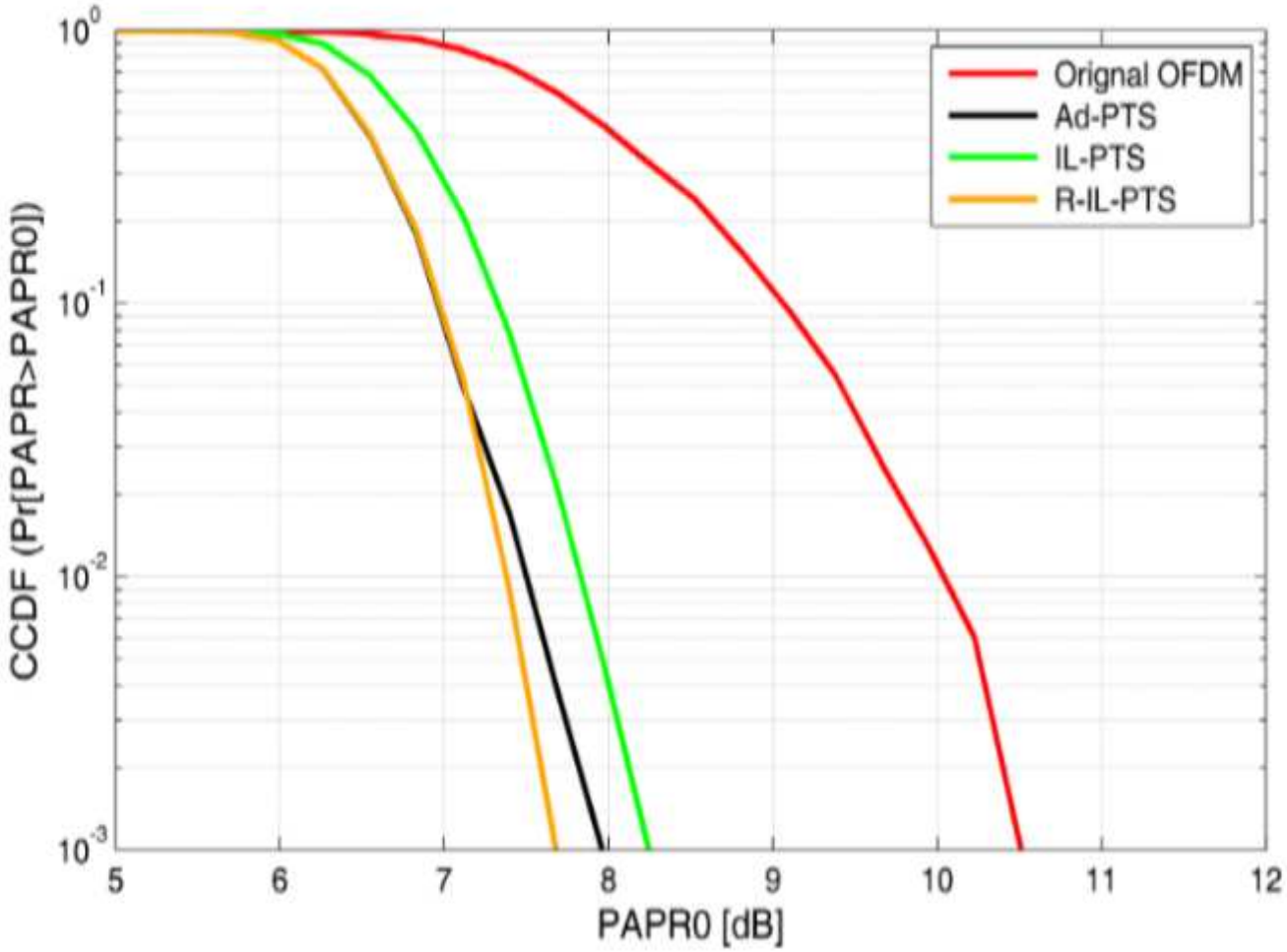

Figure 10

Comparison R-IL-PTS, IL-PTS and Ad-PTS, N = 128 and V= 4

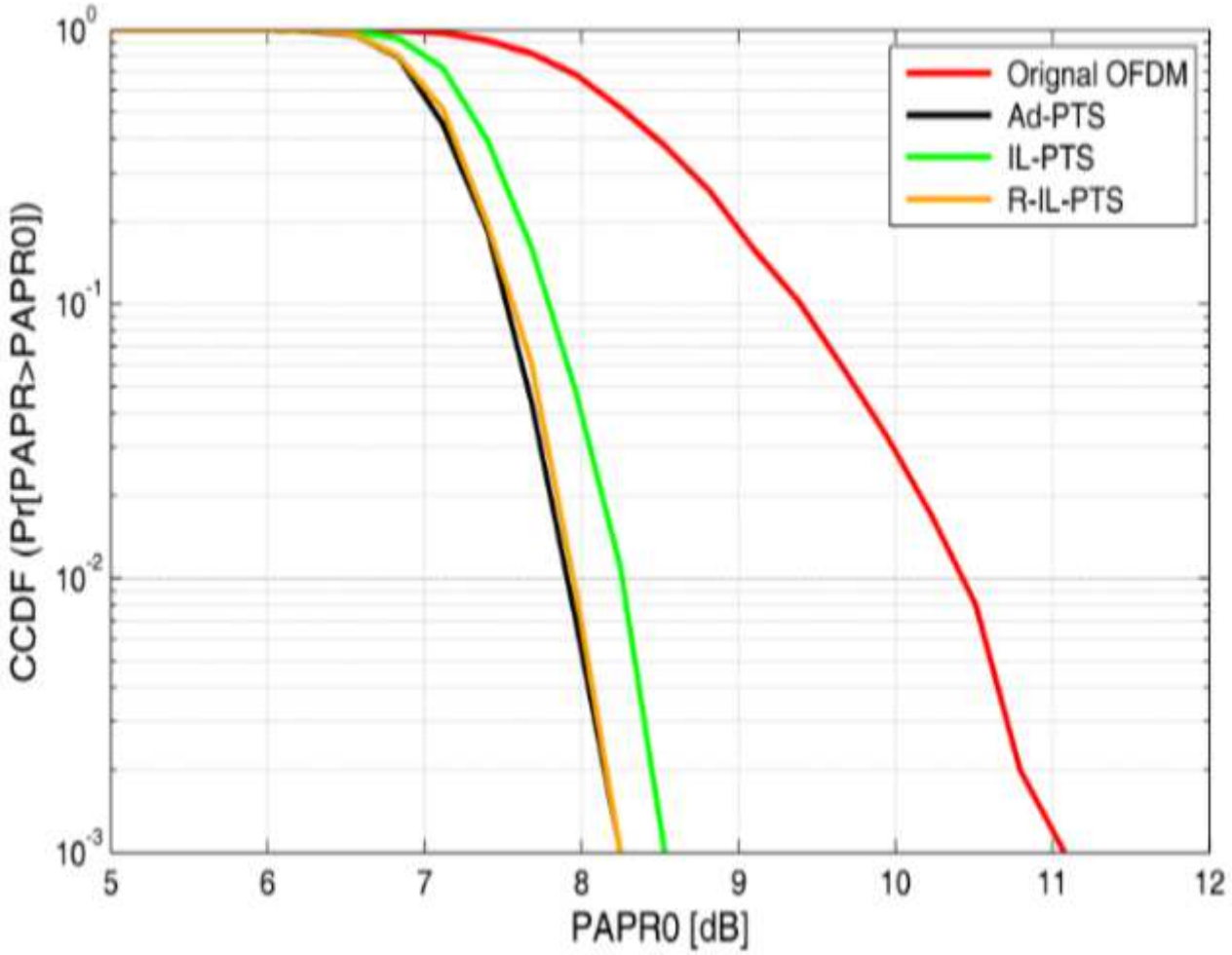

Figure 11

Comparison R-IL-PTS, IL-PTS and Ad-PTS, N = 256 and V= 4

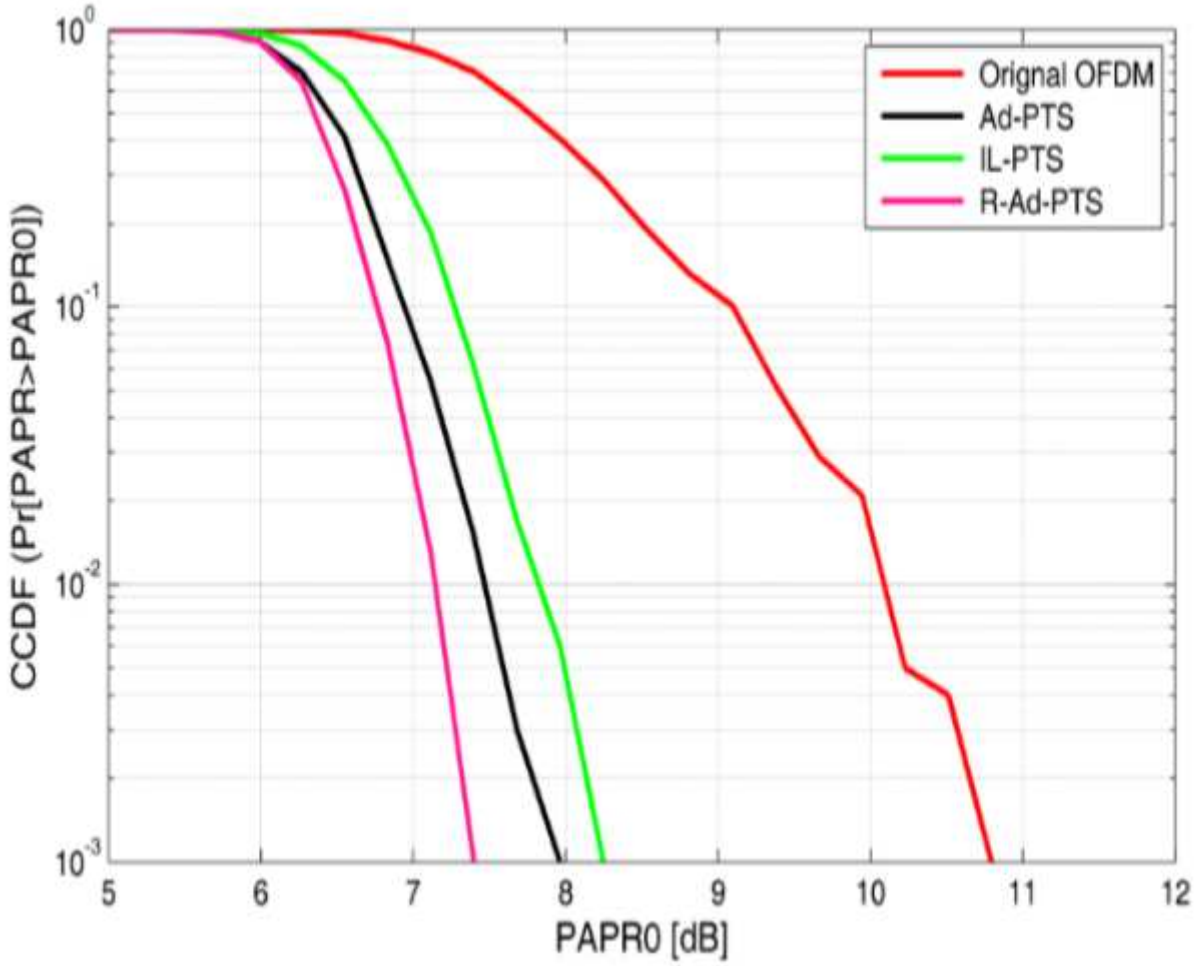

Figure 12

Comparison R-Ad-PTS, Ad-PTS and IL-PTS, N = 128 and V= 4

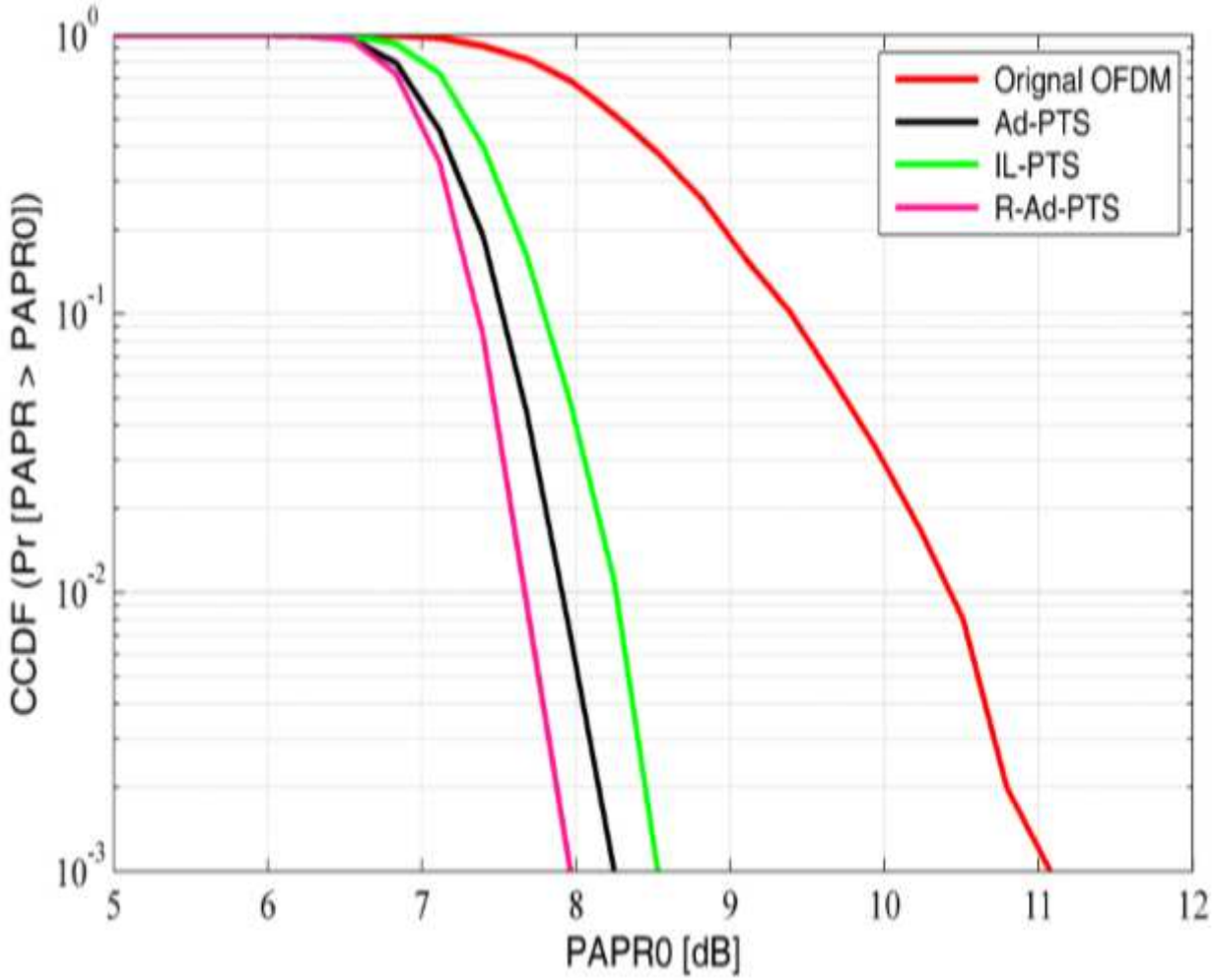

Figure 13

Comparison R-Ad-PTS, Ad-PTS and IL-PTS, N = 256 and V= 4

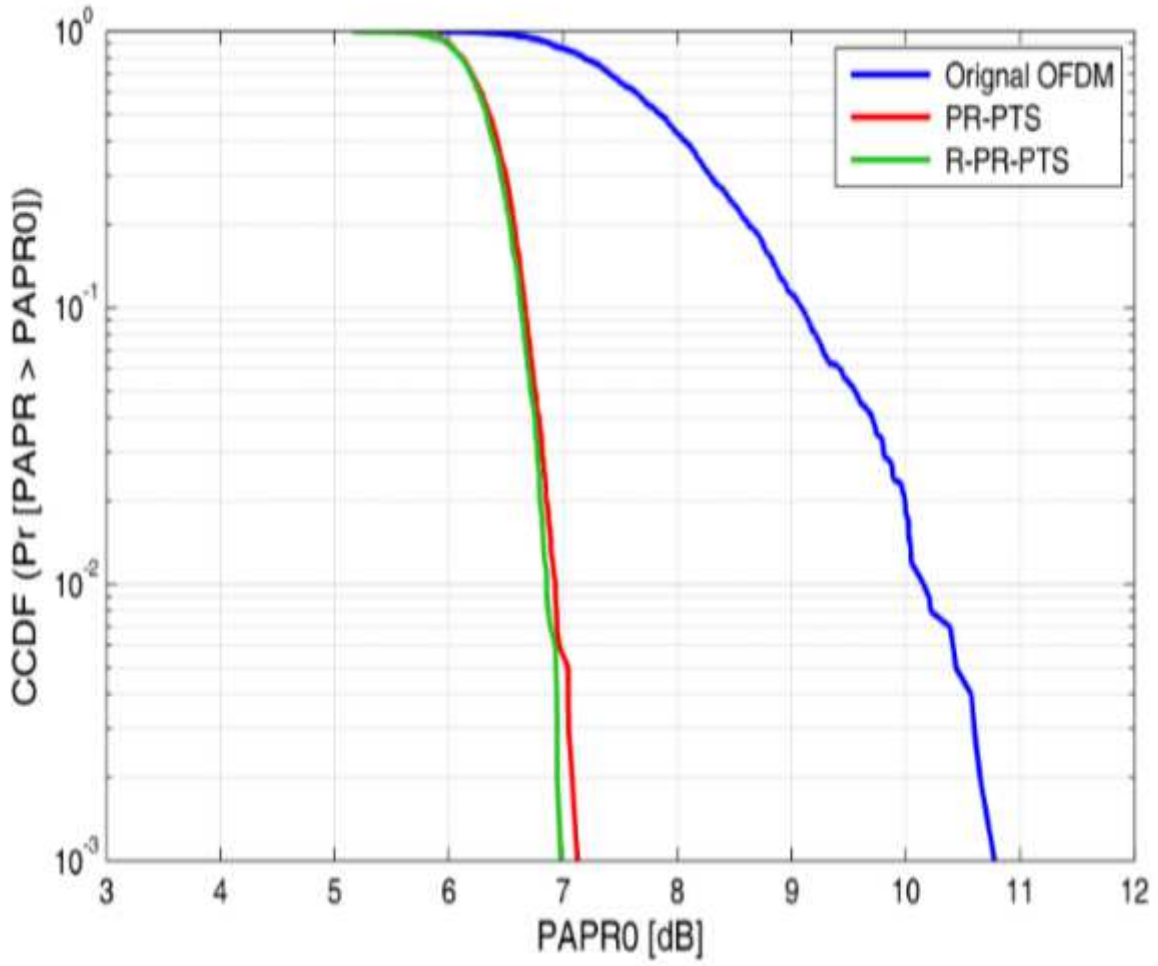

Figure 14

Comparison R-PR-PTS and PR-PTS, N = 128 and V= 4

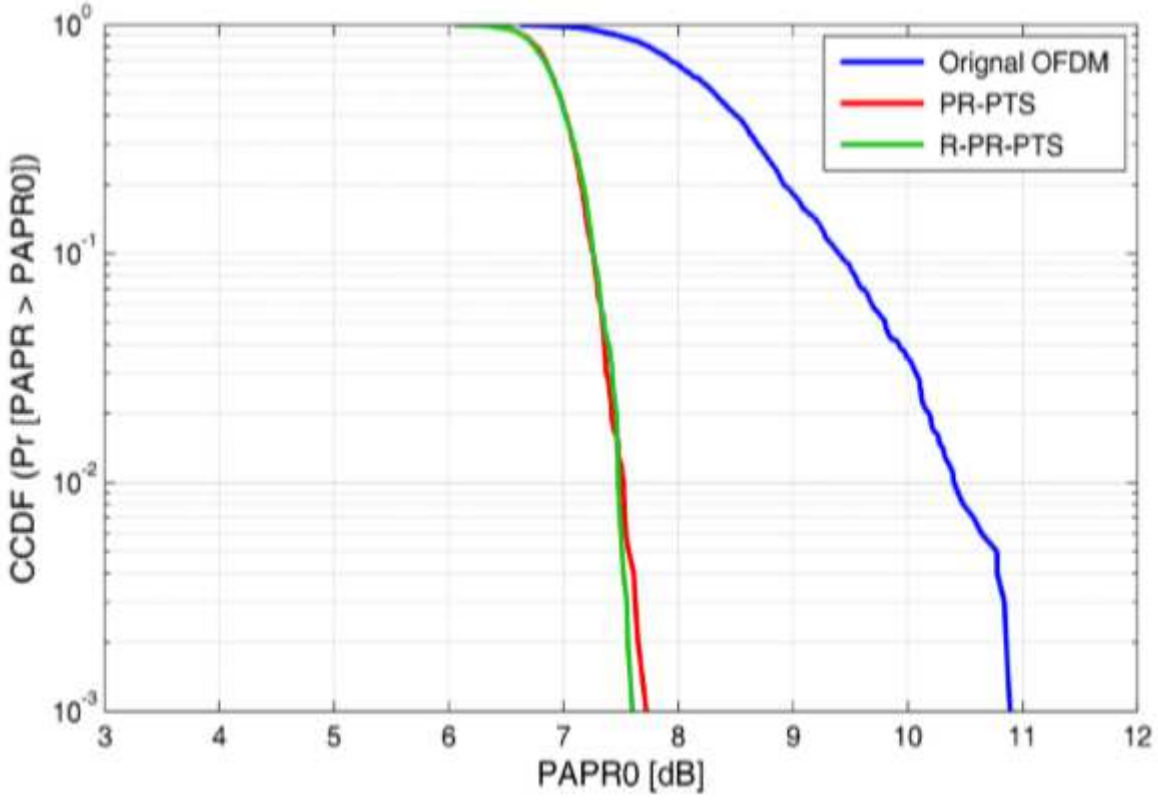

Figure 15

Comparison R-PR-PTS and PR-PTS, N = 256 and V= 4